MIT
SEA
GRANT
PROGRAM

DESIGN, DEVELOPMENT AND FIELD TRIALS OF A TOWED INSTRUMENTED GLIDER

by

K.A. Morey and E.L. Mollo-Christensen

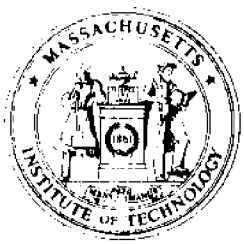

Massachusetts Institute of Technology

Cambridge, Massachusetts 02139

Report No. MITSG 76-20

November 1976

DESIGN, DEVELOPMENT AND FIELD TRIALS

of

A TOWED INSTRUMENTED GLIDER

by

K. A. Morey

and

E. L. Mollo-Christensen

Department of Meteorology
Massachusetts Institute of Technology
Cambridge, Massachusetts, 02139

Report No. MITSG 76-20
Index No. 76-320-Omn

Authors

Erik L. Mollo-Christensen is a professor of meteorology in M.I.T.'s Department of Meteorology.

Kenneth Morey is an engineering assistant in M.I.T.'s Department of Meteorology.

Related Publications

Masubuchi, Koichi. MATERIALS FOR OCEAN ENGINEERING. Cambridge: M.I.T. Press, February 1970. 542 pp. $14.50.

Abkowitz, Martin A. STABILITY AND MOTION CONTROL OF OCEAN VEHICLES. Cambridge: M.I.T. Press, May 1969. 352 pp. $15.00.

Mandel, Philip. WATER, AIR AND INTERFACE VEHICLES. Cambridge: M.I.T. Press, April 1969. 202 pp. $9.95.

Note

The preceding publications may be ordered from Communications, M.I.T. Sea Grant Program, Room 5-331, Massachusetts Institute of Technology, Cambridge, Massachusetts 02139.

ABSTRACT

This report describes the design, construction and field use of an underwater glider that functions as an instrument platform designed to be towed behind a ship. The glider is towed on a constant length cable with descent and ascent controlled by hydrodynamic lift on wings and control surfaces. An electronic feedback system enables the glider to maintain constant depth and to respond to commands for prescribed depth variation. The glider in the tests reported, carried temperature, depth and electrical conductivity transducers. The towing speed range was four to ten knots, with a depth range 0 to 100 feet. Sample data from exploration of the oceanic surface layer are also included.

PREFACE

The development of the towed instrument system described in this report was started under NOAA-Sea Grant sponsorship; it was later continued with support from NOAA under Contract NAS 8-28922. The construction of the second prototype was supported by ONR under Grant N00014-67A0204-0024. The sensor system in the present prototype was built with support by the same ONR Grant. Field trials and participation in the GATE Experiment were carried out under NSF Grant No. DES71-00324.

Many colleagues and associates made valuable suggestions and contributed useful critcism. D.G. Strimaitis participated in field trials, calibration, final adjustment and GATE III observations. His contributions are acknowledged with thanks. D. Crary, research engineer, developed the initial control servo system. The conductivity-temperature-depth package was built with help and advice from Neil Brown of Woods Hole Oceanographic Institute and Prof. R. Beardsley and E. McCaffrey of M.I.T.

The towed package and instrument system were planned to fit into a larger navigational-course control-interactive data acquisition system as described in Reference(1).

---

(1) Department of Meteorology, M.I.T.; Lincoln Laboratory, M.I.T.; C.S. Draper Laboratory, Inc. (Prepared by), C-4089 Final Technical Report of Phase I Activities in the Development of a Dynamic Scanning and Data Acquisition System for the Observation and Interpretation of Environmental Dynamics, November, 1973. Available from C.S. Draper Laboratory, Inc.

TABLE OF CONTENTS

FIGURES

Appendix II Illustrations

Page

Appendix III Illustrations

1.0 Introduction

In the upper few hundred meters of the ocean and within the thermocline, the horizontal variability in temperature, salinity, velocity and density is significant over scales of a few depths. This variability affects all variables, be they physical or biological.

Whether one's goal is to establish meaningful averages or explore the dynamics of the phenomena that cause the variability, one needs a high horizontal density of observations.

An instrumented buoy, capable of taking observations closely spaced in the vertical direction, and placed in a current, will provide many profiles of the water mass drifting by. A towed probe, capable of taking vertical sections as well as being towed at constant depth would be a valuable complement to buoy observations and ship's stations.

The towed sensor platform-sensor package described in this report does not involve automatic navigation, course control and interactive data logging and display systems. These aspects of a projected ultimate system are dealt with and reported on by the C.S. Draper Laboratory, Inc., in Report C-4089.

This report covers a description of what has been called, for internal lab purposes, the Mark II Hydroglider System; its intended use, the design targets and design of the system at its present stage of development. Before describing the present system, the report discusses general features of other systems for cable depression and other towed instrument platforms.

2.0 Other towed instrument systems

The choice to go ahead and develop a new towed instrument package was based on an examination of available systems, first when the development was started in 1972 and later, in 1973, when it was decided to continue in spite of the appearance of other systems in the literature and on the market.

The sales literature and available descriptions of non-controllable towed bodies and cable depressors were first examined. While all of these, from delta-shaped hydrodynamic cable depressors to streamlined weights with fins for alignment with the towing line, served their intended specific purposes, they provided no means for maintaining constant depth. Neither did they provide means for compensating for heave of the towing vessel or means for programming depth changes without winch operations. The most sophisticated system in this class is the "Fathom" system, which consists of a combination of a streamlined heavy body, a streamlined cable and a winch system with provisions for depth control, cable tension control and other desirable features.

A depressor which relies on weight to compensate for hydrodynamic forces on a cable may work well over a limited speed range. However, since hydrodynamic forces vary as the square of the velocity through water and gravity forces remain independent of speed, the geometry of a cable-depressor combination will change with towing speed. For high towing speeds, large weights will be needed to keep the cable end at

desired depth; at low speeds, a smaller weight is required. For large submerged weights, large winches are needed for deployment. While such systems may be highly suitable for special uses, it appeared desirable to have a system which was not dependent upon winches to change depth, especially for deployment from a small vessel.

Inert hydrodynamic depressors, such as V-fins and airfoil cascades, although valuable for many purposes, leave a need for more flexible designs through use of controlled hydrodynamic depressors.

The "Batfish" was also considered; this is a hydrodynamic depressor with variable incidence main lifting surface, actuated through electric commands to a hydraulic actuator system, and roll stabilized through a high-set fin rudder actuated by a weight with center of gravity astern of the center of lift of the fin. We were aware of the many problems that are involved in design of delta wing aircraft for satisfactory stability, as well as the possibilities for coupled lateral and longitudinal oscillations of aircraft with significant cross-moments of inertia or of aerodynamic coefficients. The present designs of vehicle-cable combinations for the Batfish no doubt perform well, and according to specifications.

In view of the likely sensitivity to changes in geometry and mass distribution, a vehicle less sensitive to payload configurations and stable very near the surface as well as at depth would be highly desirable. These considerations were among those that prompted the development of the hydroglider.

3.0 Design targets

The goal was to design a towable instrument platform controllable in depth without hoisting or lowering cable from the towing vessel. The system should be minimally capable of carrying conductivity-temperature-depth instrumentation and leave room for the inclusion of other sensors with future development. As an additional feature, it was decided to allow for the placement of sensors along the towing cable for observation of small scale vertical gradients while towing horizontally. This feature also allows a more direct integration with the dynamic scanning system being designed by the C.S. Draper Laboratory, Inc.

A set of vertically spaced sensors will also allow one to use the system to locate the boundaries between water masses, be the boundaries horizontal or vertical, and to place probes on both sides of the boundary for further exploration. The types of phenomena and processes kept in mind during the system design are the following:

--Exploration of boundaries between water masses, from the continental shelf edge front to the limits of jets emitted by harbors and channels,

--The capability to trace estuarine mixing processes, and near surface processes of vertical mixing and advection,

--Observation of internal-inertial and topographic wave phenomena.

By keeping these targets in mind, excessive specialization was avoided. An oceanographer, developing an instrument needed in a research problem, tends to specialize the instrument for one particular

purpose. This often makes the instrument of little use in the exploration of other processes. The system described here is relatively simple and may turn out to be a useful tool for a variety of oceanographic observations.

During the initial period of Hydroglider development the prevailing attitude has been that worthwhile data collection on a prototype system is of far more value than the design of a hypothetically perfect system incorporating new technology, although months from implementation. This concept was expanded to include initial simplicity, reliability, modular construction and rapid development of both the control and instrumentation systems. The end product of this line of reasoning has been the development of a stable, controllable instrumented towed platform, successfully used in the GATE Experiment.

The decision was made to design, develop and field test an analog servomechanism for control and include the necessary elements in the system to interface to existing instrumentation modules.

One of the first problems encountered in development of the electronic control sytem was how to monitor and make the necessary scaling adjustments of the electronics during initial trial periods. This problem was solved by locating the control logic electronics on the towing vessel as on-board equipment. Only the mechanical controller package consisting of the motor, angular sensing potentiometer, and mechanical linkage to the glider control surface was located on the Mark II. It was felt that the adverse effects of separating the control logic elec-

tronics from the mechanical controller and controlled surfaces would be far outweighed by the convenience of the adjustment and modification of on-deck components.

To facilitate system development and the repair of electronic and mechanical malfunctions, as well as to simplify system operations, both electronic and mechanical elements were designed in modular form.

4.0 Overall description of the system

The system consists of the glider, the sensor packages, the elevator actuator package, the power supply package, the towing cable, the ship-board glider control system and the data recording system, as illustrated in Fig. 1.

In Fig. 2, the glider, cable and depth control system are represented in terms of a block diagram. The figure illustrates that the glider and cable dynamics are part of the system, that this dynamics changes with parameters such as sea state and towing speed. A depth command, be it a constant or programmed variable depth signal, is provided by the depth command generator. The depth of the glider is sensed by a pressure transducer and the resulting depth error signal is processed to generate an elevator command; the elevator deflects,modifying the glider angle of attack, generating lift and thereby causes the glider to ascend or descend, bringing the glider-cable configuration into a new state of equilibrium.

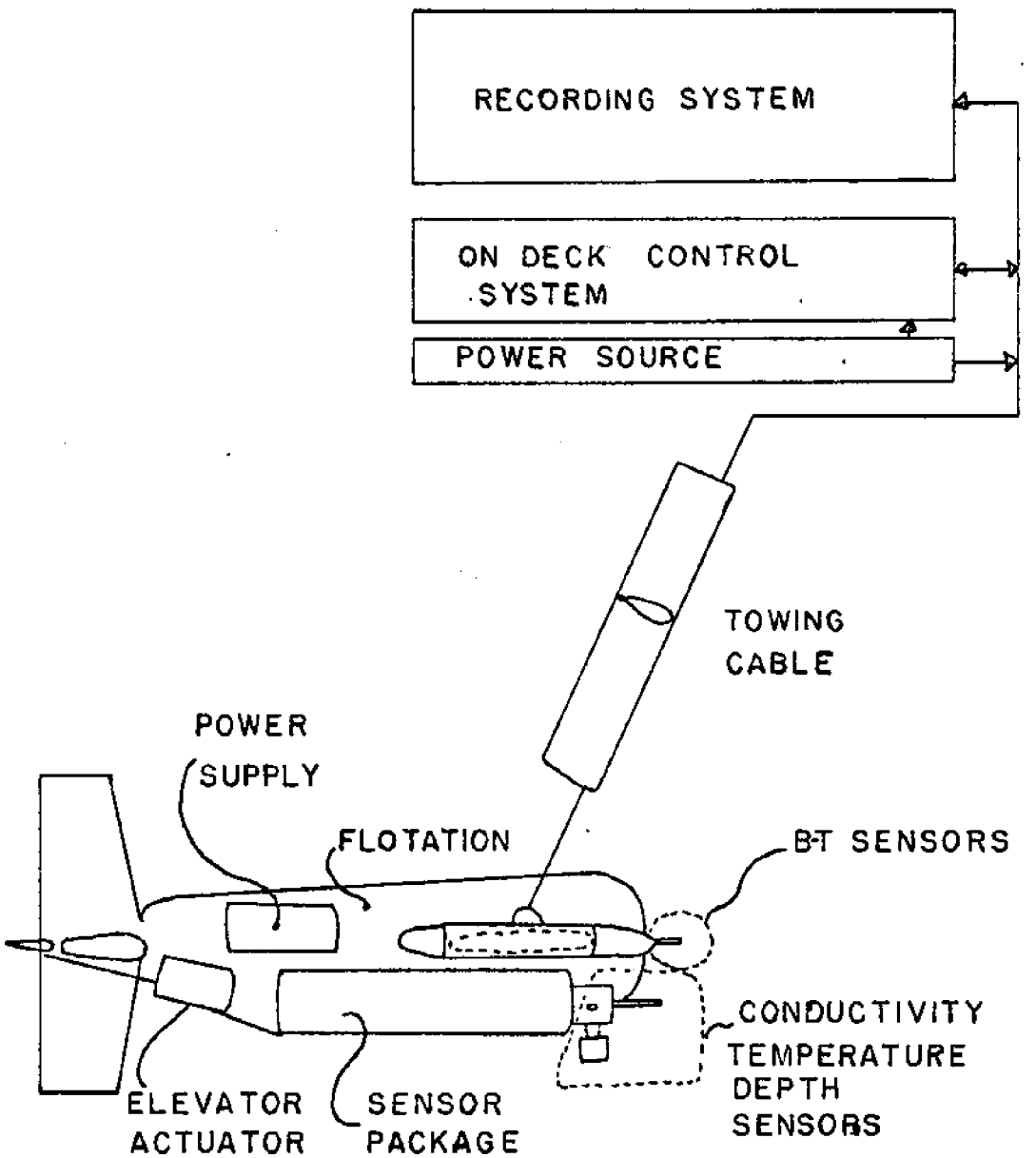

FUNCTIONAL SCHEMATIC

FIG·1

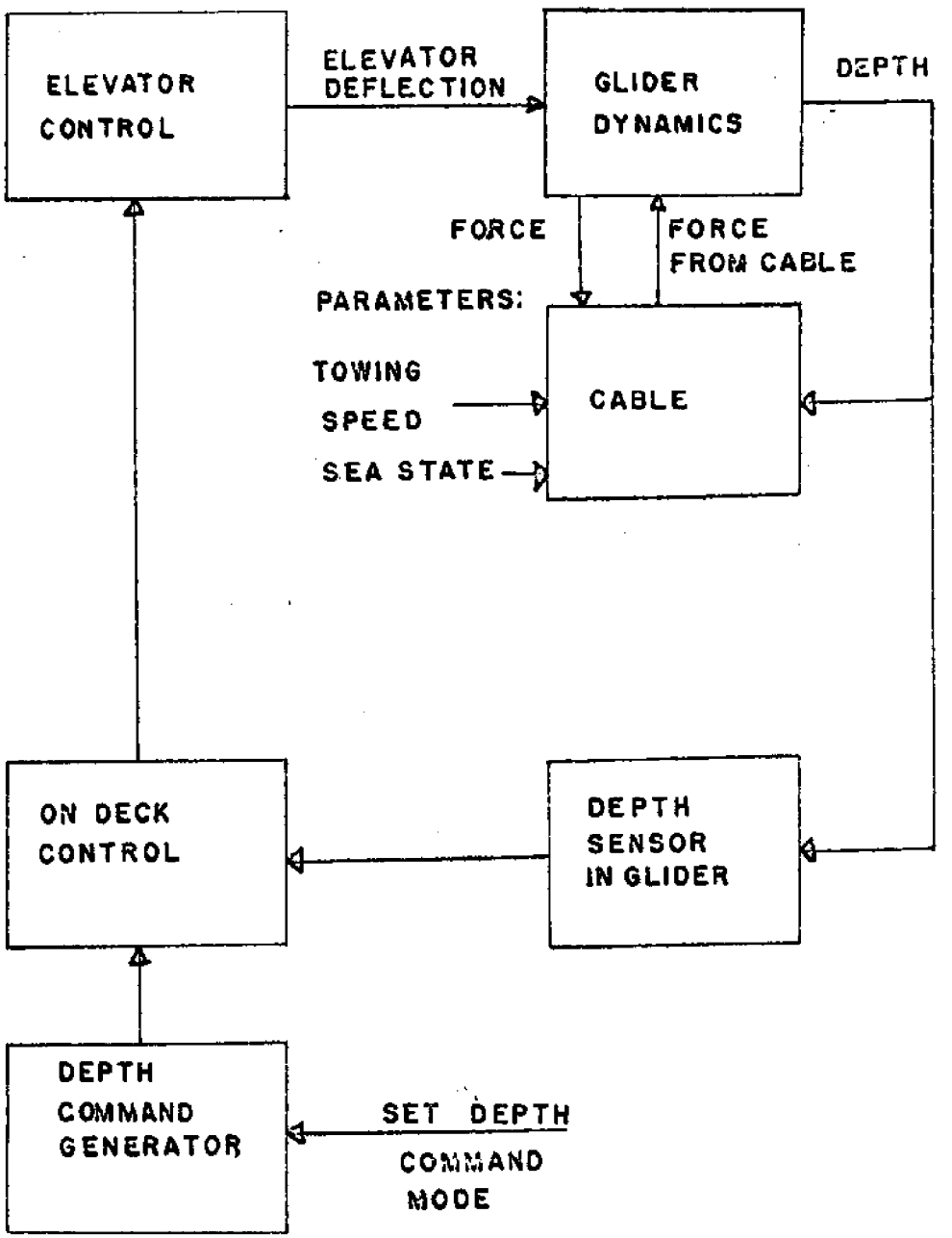

GLIDER- CABLE DYNAMICS AND DEPTH CONTROL BLOCK DIAGRAM

FIG·2

We proceed to describe the parts of the system in terms of the hydrodynamic design, the structural design, and the control system design.

5.0 Hydrodynamic design

The hydrodynamic design draws on low-speed aircraft design experience. The Reynolds number of the glider is approximately 2×10^6, based on wing chord, while the Reynolds number of a light aircraft is of order 10^7. Both these Reynolds numbers are above the critical value for boundary layer transition, and the flows are similar. One can therefore copy small aircraft design practice without encountering new problems with stall and boundary layer separation characteristics. The restrictions on structural weight were much less severe than for aircraft; there was little need to optimize the design for low weight or low power requirements. The design attempts to follow some of the maxims of light aircraft design, trying for:

(1) Low wing loading, to avoid operation near stall where lateral stability may be hard to maintain.

(2) Large effective wing aspect ratio--the present design uses tip-tanks to make the flow over the wing more two-dimensional, so as to increase effective aspect ratio.

(3) Plenty of vertical tail area and large tail length to improve lateral stability, alleviate spiral instability and yaw-roll-pitch instability with coupling to cable dynamics.

By following these guidelines, one has a good chance of ending up with a stable system without having to go through a complicated dynamic nonlinear stability analysis. In addition it was decided to make the glider nearly buoyant to simplify recovery and minimize chances of getting caught in the ship's propeller while stopped. Also, if something should go wrong, it is nicer to have the glider float than sink.

An overall view of the glider with towing bridle attachment is shown in Fig. 3. Fig. 4 is a three-view of the glider; Fig. 5 shows the hydrodynamic surfaces in isolation, and the hydrodynamic characteristics are tabulated in Table I.

In order to estimate drag and lift for structural design purposes and to obtain crude estimates of performance, a parasitic drag coefficient of $C_{DP} = 0.10$ and a maximum lift coefficient $C_{Lmax} = 1.4$ were used. Adding the induced drag coefficient, one finds a drag, D, and lift, L, to be:

$$D = C_D \cdot 1/2\rho U^2 \cdot A$$

$$L = C_L \cdot 1/2\rho U^2 \cdot A$$

where:

$$C_D = C_{DP} + \frac{C_L^2}{\pi AR};$$

$$C_{Lmax} = 1.4; \quad C_{Dmax} = .256$$

$$C_{LP} = 0.10$$

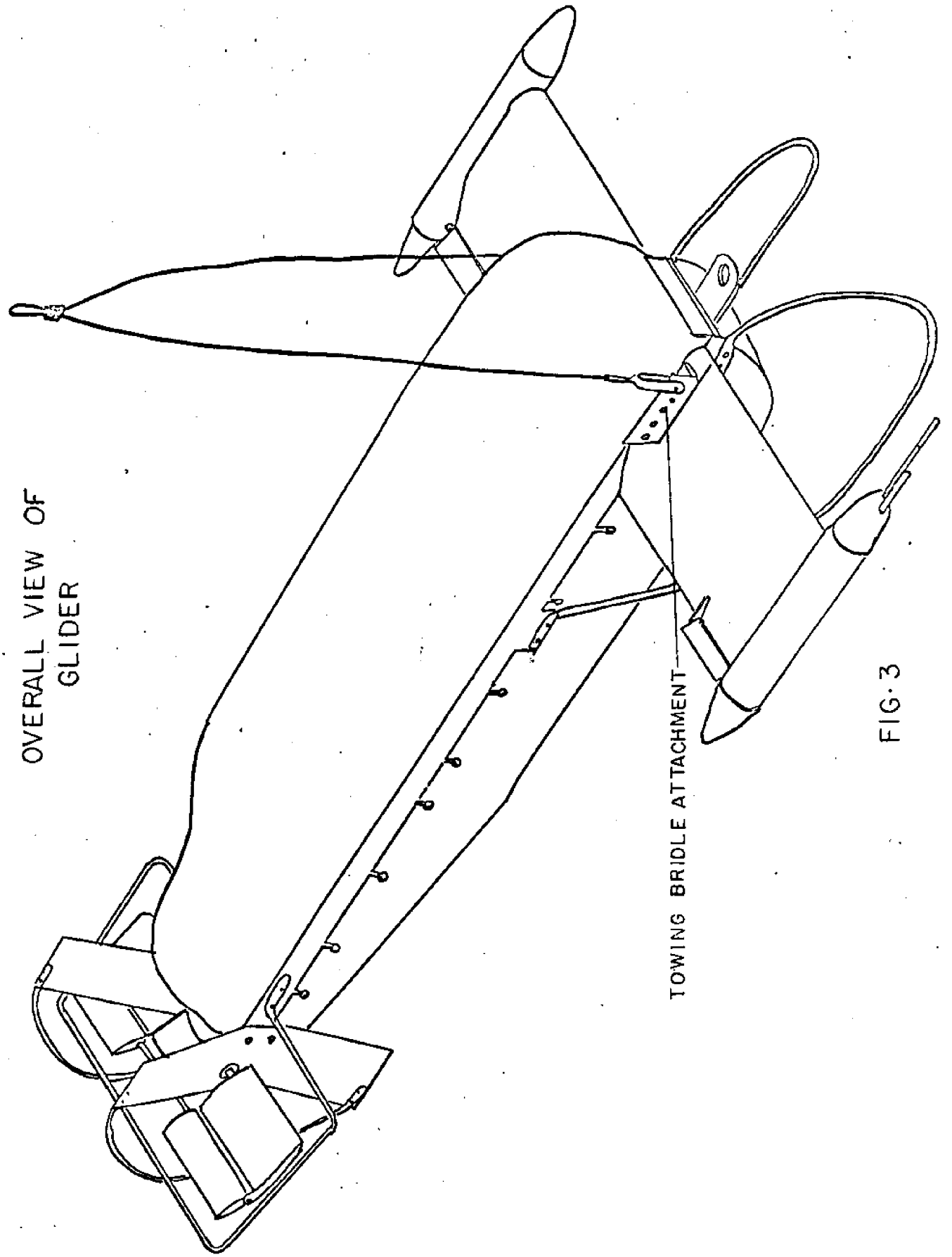

OVERALL VIEW OF GLIDER

FIG·3

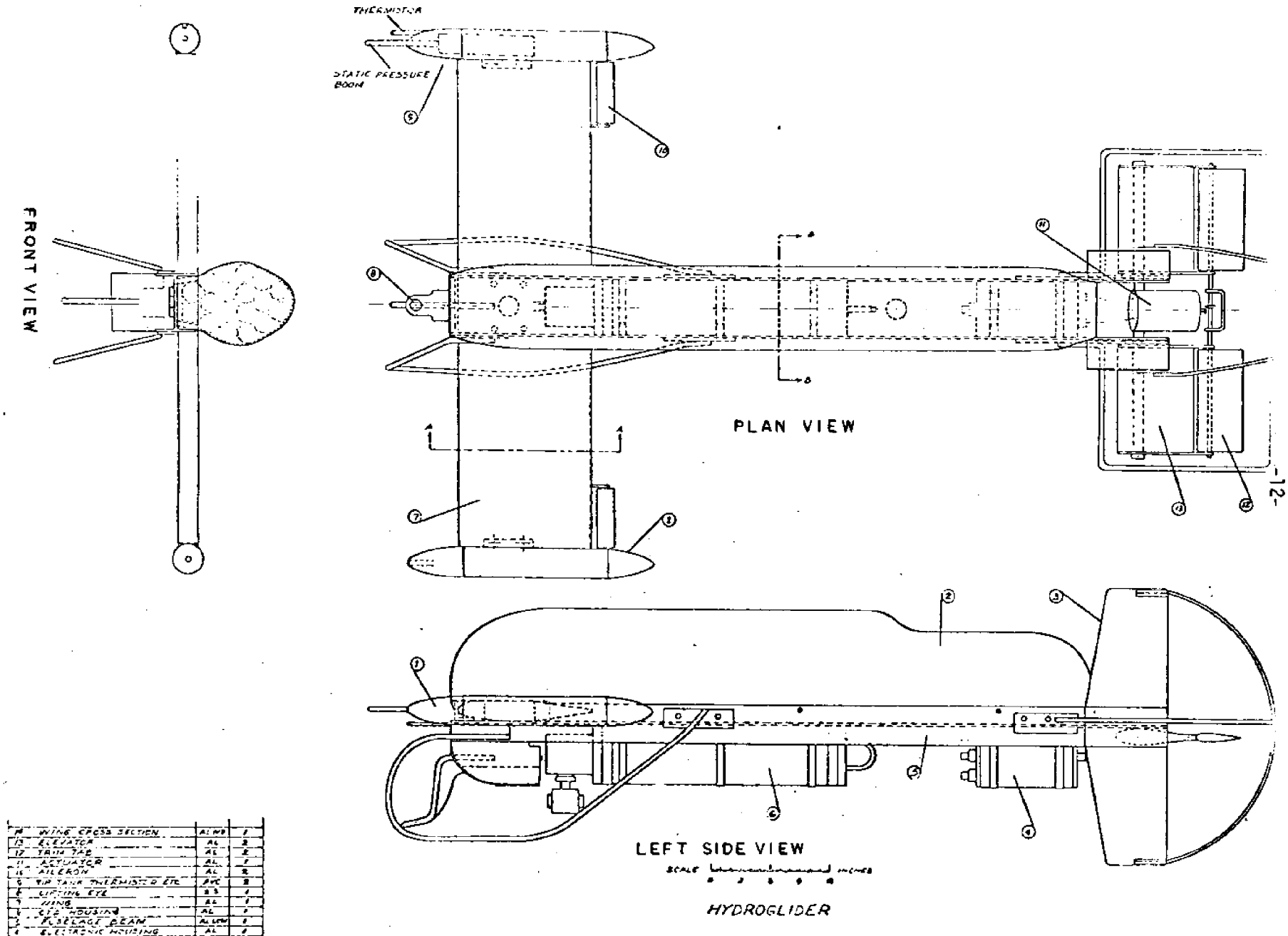

14	WING CROSS SECTION	ALMG	1
13	ELEVATOR	AL	2
12	TRIM TAB	AL	2
11	ACTUATOR	AL	2
10	AILERON	AL	2
9	TIP TANK THERMISTOR ETC	PVC	2
8	LIFTING EYE	S.S.	1
7	WING	AL	1
6	C.G. HOUSING	AL	1
5	FUSELAGE BEAM	AL ALLOY	1
4	ELECTRONIC HOUSING	AL	1
3	VERTICAL FINS	AL	2
2	FUSELAGE BODY	PLASTIC	1
1	TIP TANK	PVC	2
	PAL		

FIG·4

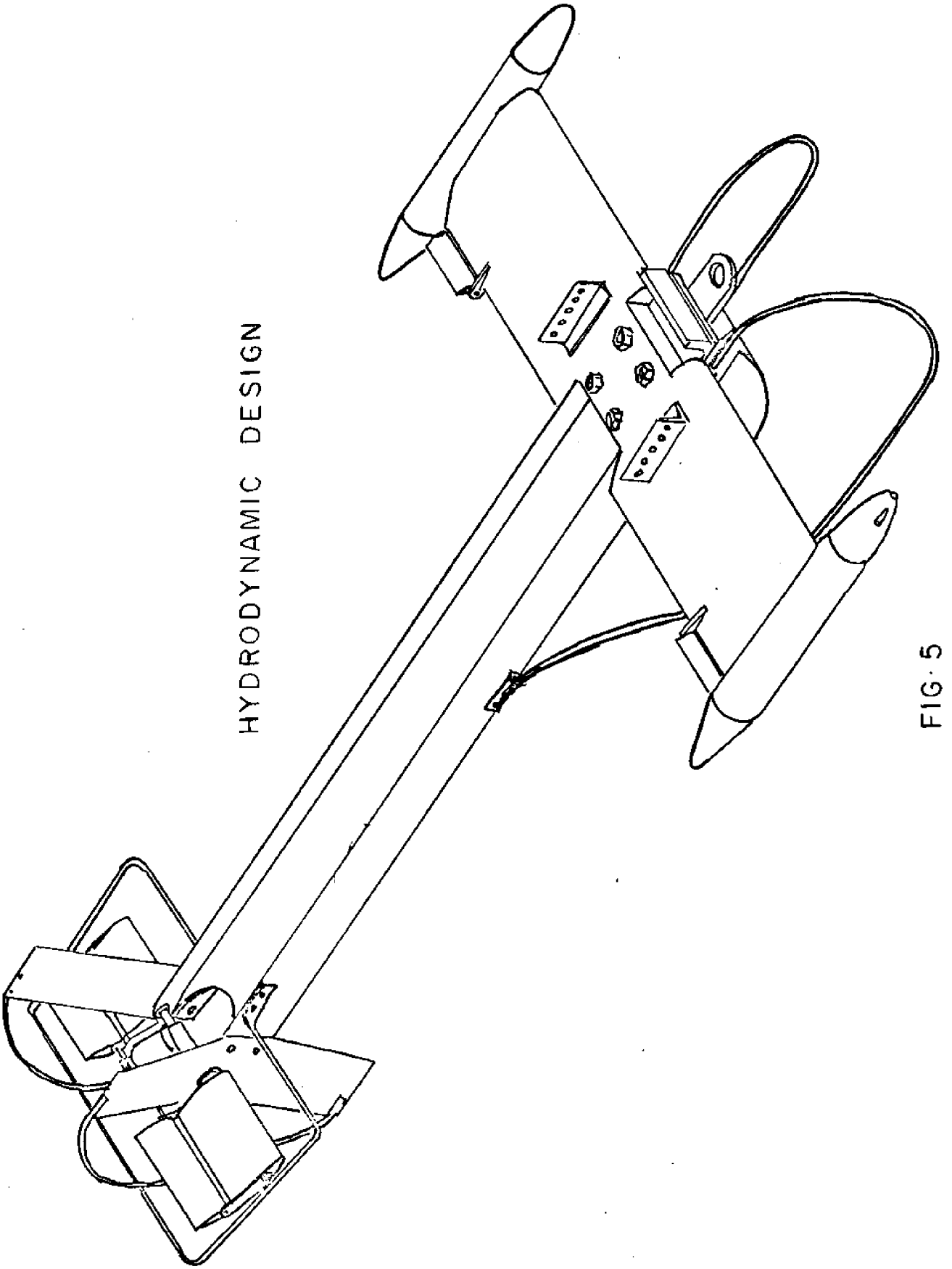

FIG. 5

Table I

Wing area	4.5 ft^2	=	0.414 m^2
Wing span	4 ft	=	1.20 m
Wing chord	13.5 in	=	0.338 m
Aspect ratio	3.55		
Ailerons:			
Span	6 in	=	15.24 cm
Chord	1.25 in	=	3.17 cm
Fraction of semispan	1/8		
Area	7.5 in^2	=	48.4 cm^2
Vertical stabilizer:			
Area	1.36 ft^2	=	0.125 m^2
Height	28 in	=	0.71 m
Average chord	7 in	=	17.8 cm
Distance from wing hydrodynamic center approximately:	1/4 chord to vertical fin		
	69.4 in	=	1.763 m
Rudder	none		
Horizontal tail:			
Total area	1.103 ft^2	=	0.101 m^2
Distance from wing stabilizer 1/4 chord:	1/4 chord to horizontal		
	70 in	=	1.78 m
Elevator (servo elevator) area:			
	0.325 ft^2	=	0.029 m^2
Weight in air	175 lbs	=	79.5 kg
Buoyancy	200 lbs	=	90.8 kg
Excess buoyancy	25 lbs	=	11.4 kg

$\mathcal{R}$ is the aspect ratio of the wing. In view of the presence of the tip tanks a value of R = 4 has been used.

Table II shows estimated maximum lift and drag at towing speeds of 1 m/sec, 5 m/sec and 8 m/sec.

Table II

Maximum estimated lift and drag

Towing speed		Maximum lift		Maximum drag	
m/sec	knots	kg	lbs	kg	lbs
1	1.94	30.4	67	5.56	12.3
5	9.72	761	1,676	139	306
8	15.55	1,947	4,288	356	784

These estimates served as a basis for the structural design of the wing and for selection of cable strength specifications.

In the hydrodynamic design it will be noted that the tail extends upwards and downwards, to give directional stability when the wing is stalled either way. It will also be noted that there is no wing dihedral. Dihedral gives yaw-roll coupling, but for flight at both positive and negative lift, dihedral will only improve stability for one sign of lift and make stability worse the other way. The fairing shell over the instrument housings serves to lower the drag.

The elevator actuator is shown in Fig. 6. An electric motor, enclosed in a cylindrical housing with a packing gland at the drive shaft, drives a set of bevel gears that rotate the control surface.

The ailerons are not coupled. Each aileron is deflected independently by a pendulum weight placed in the tip-tank (Fig. 7). The pendulum has an overtravel stop, so that, if the glider is inadvertently turned upside down during deck-handling or launch, the ailerons will not lock in a deflected position. When the glider rolls away from horizontal, the ailerons deflect so as to bring the roll angle back to zero. The system works well.

Towing bridle attachment. The towing bridle attachment is shown in Fig. 8A. As can be noted, the bridle is attached approximately at 30% of the wing chord, behind the hydrodynamic center of the glider and within the estimated static margin. For downward lift, the glider should be expected to be longitudinally stable. For upward lift, when the vertical component of the force exerted by the towing cable is small, longitudinal stability requires that the center of gravity be within the static margin. This is accomplished by mounting the heaviest instrument package as far forward as possible. See Figs. 8A and 8B. The center of buoyancy, which is the other net force that affects stability, is also astern of the hydrodynamic center. Although the exact locations of the center of gravity and the center of buoyancy may be fortuitous, the result is a dynamically stable glider.

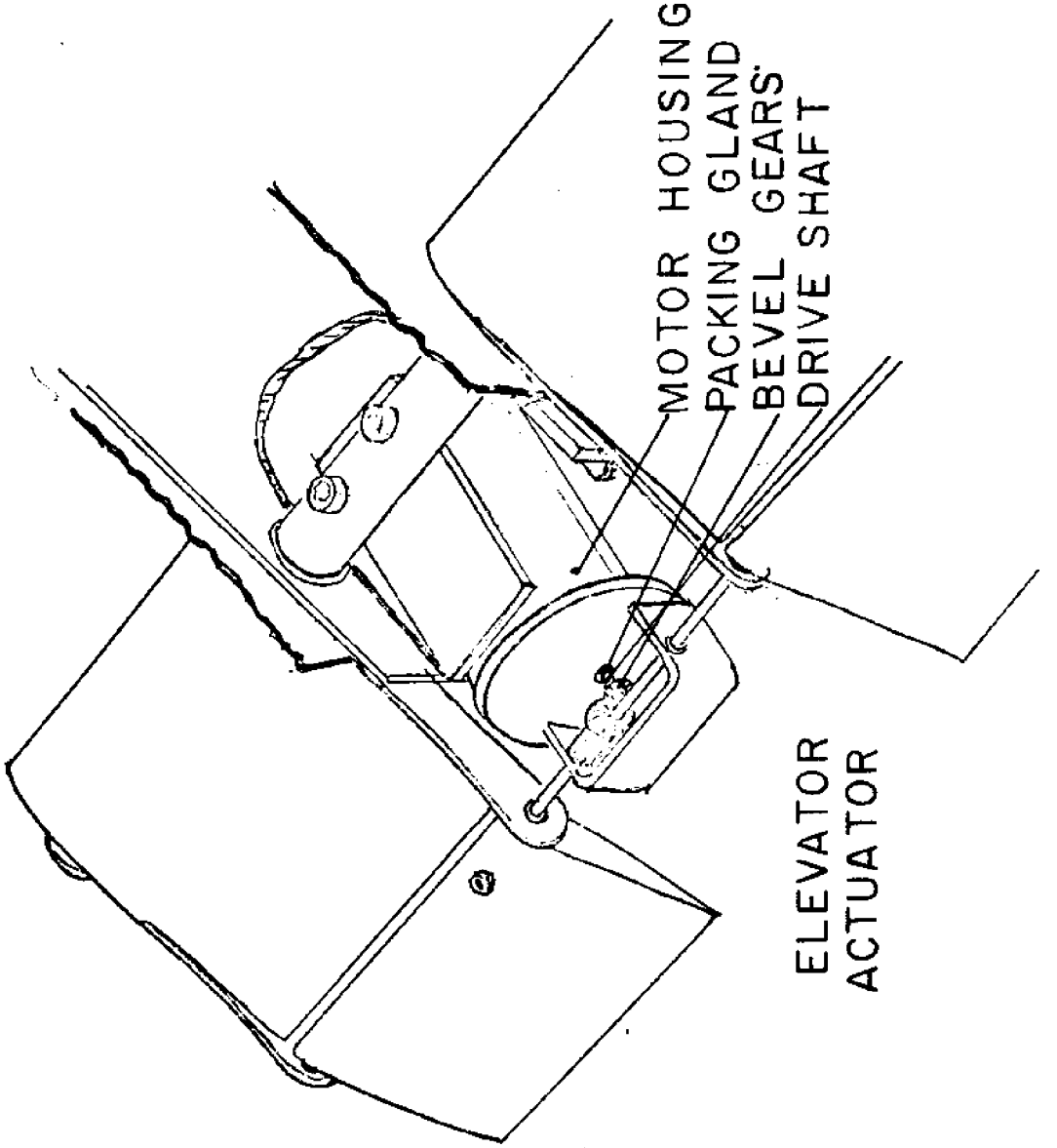
MOTOR HOUSING
PACKING GLAND
BEVEL GEARS
DRIVE SHAFT
ELEVATOR
ACTUATOR

FIG. 6

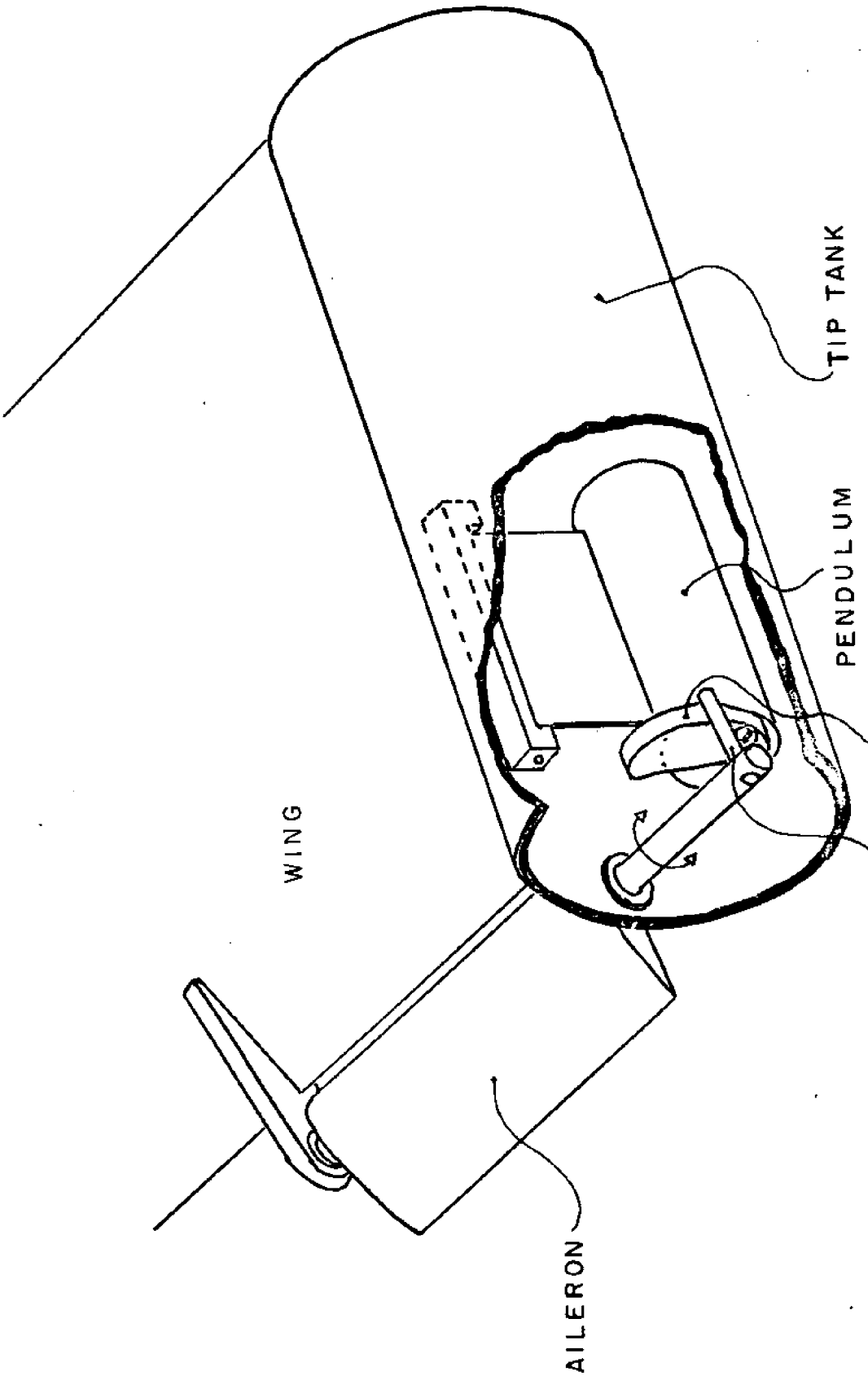

AILERON CONTROL

FIG. 7

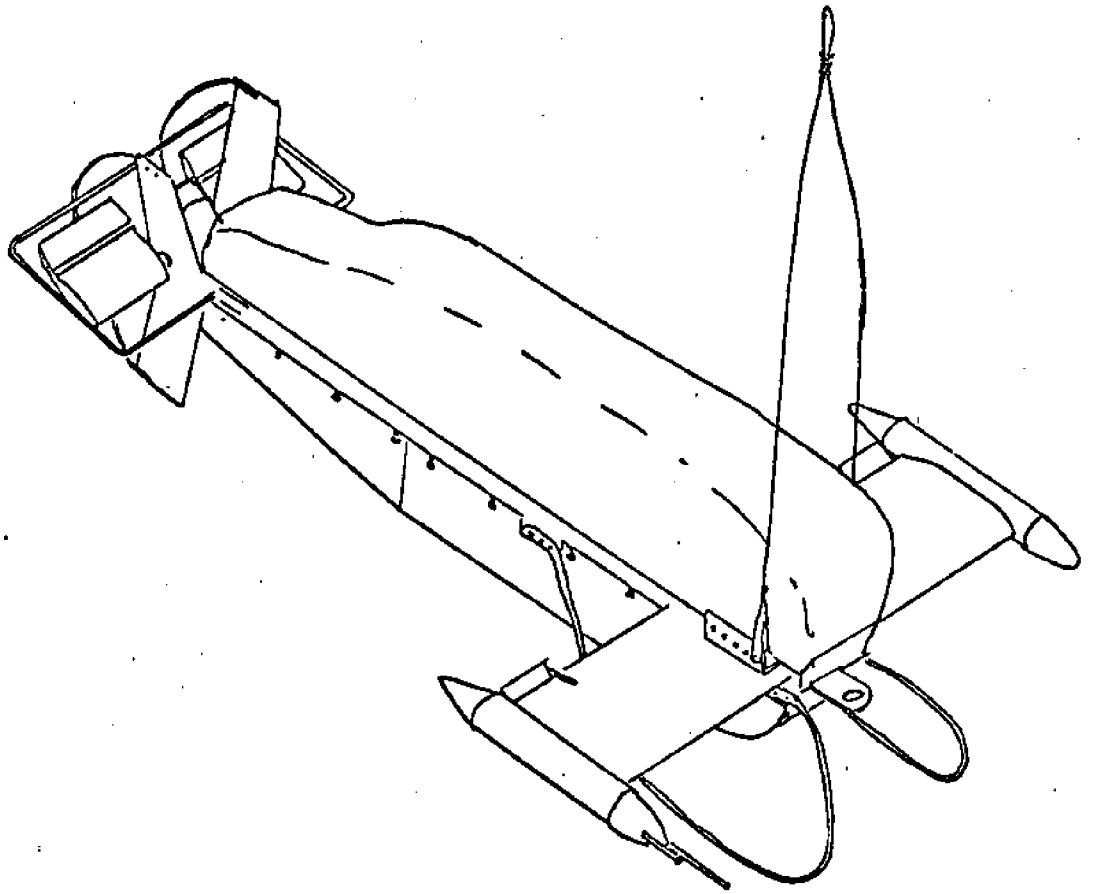

TOWING BRIDLE ATTACHMENT

FIG·8A

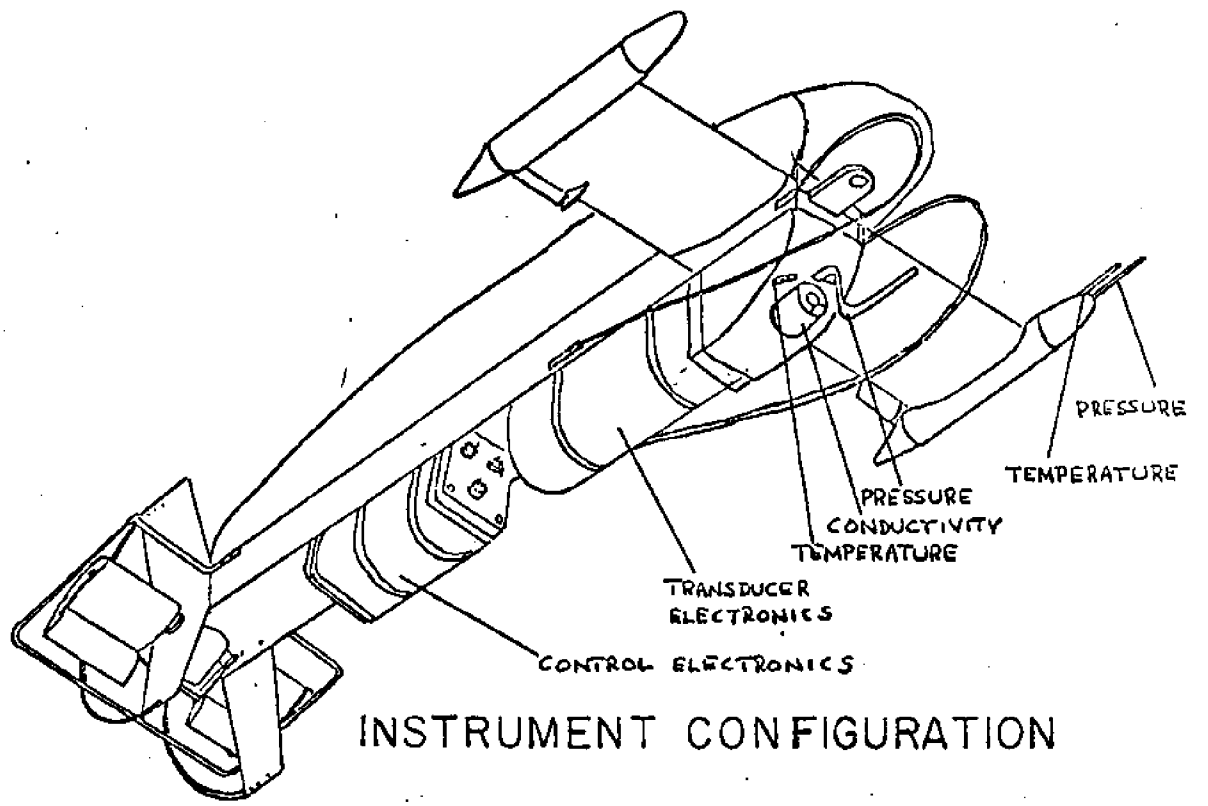

INSTRUMENT CONFIGURATION

FIG·8B

6.0 Ascent limitations when towing on a streamlined towing cable

When the glider climbs, it will usually climb along a trajectory whose tangent is above or below the tangent to the towing cable at the lower end. If the glider climbs at a sufficiently steep angle so that it pulls the end of the towing cable upwards, the towing cable will be moving "backwards". A streamline fairing on the towing cable will then be moving backwards through the water and usually be hydrodynamically unstable and twist. This causes the cable to want to "kite out" laterally. The strong directional stability of the glider did prevent overall instability but the cable fairing twisted at the lower end.

For Fig. 9, it can be seen that to prevent a cable with streamline fairing from twisting, the maximum glider rate of climb is approximately

$$W_{max} = U_s \tan \Theta$$

Θ is the angle between the horizontal and the tangent to the cable of its lower end; U_s is the speed of towing.

For cable with a circular cross-section or a cable with non-directional fairing, this limitation does not apply. This limitation is only severe near the water surface, where Θ is small. Operating at depth, such that, for example, $\Theta_{min} > 30°$, the limitation on W is

$$W_{max} = U_s/2.$$

In view of this, we recommend that the glider be used with a towing cable with non-directional streamline fairing and that a cable with rigid fairing be used with limit stops on the rate of climb command signal.

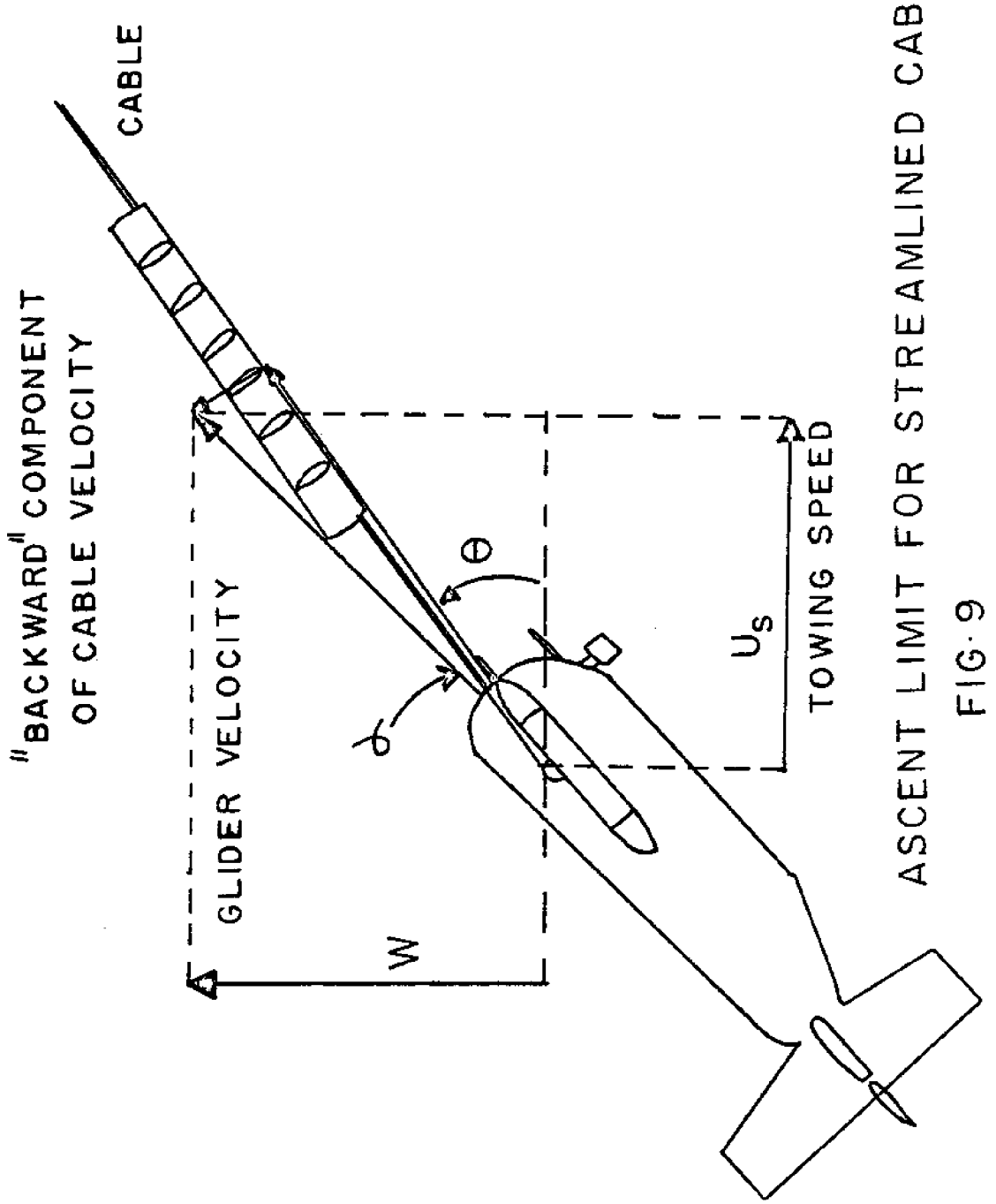

ASCENT LIMIT FOR STREAMLINED CABLE TOWING

FIG. 9

7.0 Structural design

Fig. 10 shows the basic structure, the fuselage H-beam, the wing rectangular box beam and the 3/4 inch stainless steel tube that serves as the main structural member for the horizontal tail.

The fuselage H-beam is an aluminum alloy 6061-T6 extrusion, 6 in wide with 4 in flanges by 1/4 in thick. The upper part of the flanges are cut away to accommodate the wing spar. The fuselage and the wing spar are joined using four 5/8 in dia stainless steel bolts.

Fig. 11 shows a wing cross section.

The original hollow rectangular aluminum alloy 6061-T6 extrusion is machined to 5 in X 1.75 in with 1/8 in thick at top and bottom and 1/4 in webs. A nose piece of oak is fitted and the airfoil shape produced by covering this structure by 6061-T6 aluminum skin, 0.030 in thick (0.75mm). A trailing edge stringer stiffens the trailing edge. The skin is riveted onto the spar and the trailing edge stringers using 1/8 in dia flush head countersunk rivets.

The critical design parameter is the flexural stress in the top fiber of the wing root.

At a speed of 8 m/sec and maximum downward lift, the maximum stress is found to be approximately:

$$\sigma_{max} = 13{,}400 \text{ lbs/in}^2 = 9.43 \frac{\text{kg}}{\text{mm}^2}$$

This is less than one third of the yield stress of the 6061-T6 alloy which is 45,000 $\text{lbs/in}^2 = 31.6 \frac{\text{kg}}{\text{mm}^2}$ in the T6 condition. Machining may

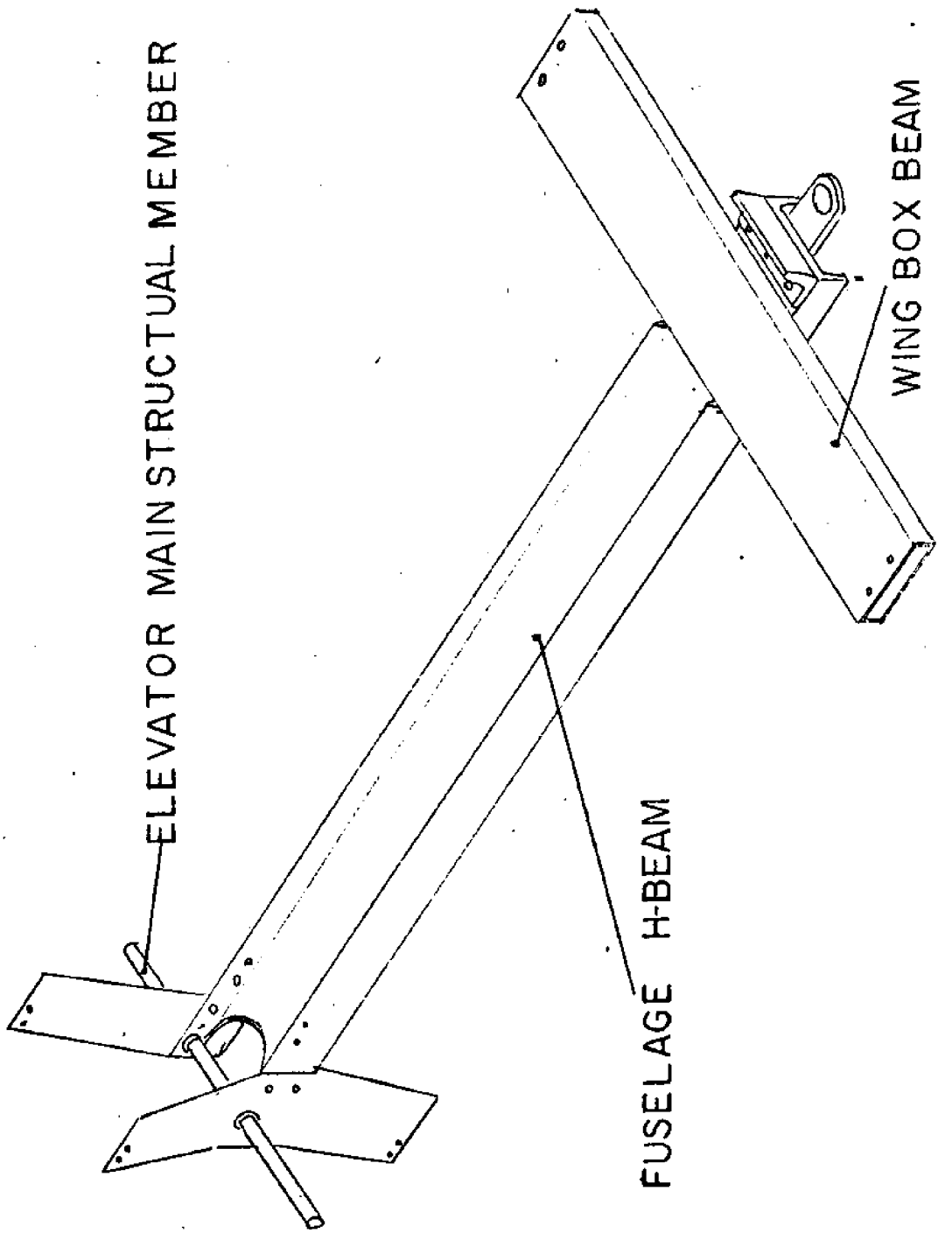
BASIC STRUCTURE OF GLIDER
ELEVATOR MAIN STRUCTUAL MEMBER
WING BOX BEAM
FUSELAGE H-BEAM

FIG. 10

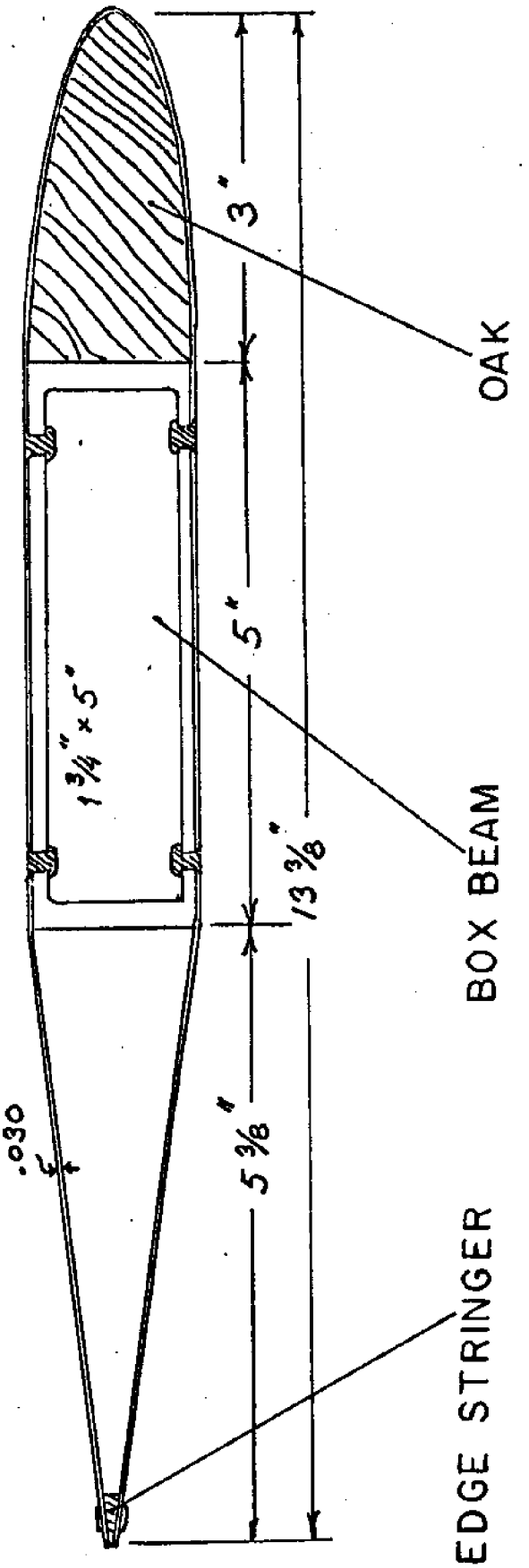

WING CROSS-SECTION

FIG-11

have lowered the temper of the box spar, and thus the yield stress. There still seems to be ample margins of safety. An additional advantage is that the reaction to the lift is not applied at the fuselage, but rather at the towing bridle; this lowers the estimated stress by twenty percent. The remainder of the structural problem was to protect the instruments and the control surfaces from being banged against the ship during launching and recovery.

This purpose was served by mounting the 3/8 in stainless steel rod skids at the front of the glider and a frame of the same material just above the plane of the horizontal tailsurface. The latter frame was joined to the top and bottom of the vertical fins by semicircular 1/4 in stainless steel rods as shown.

8.0 Functional description of the flight control system

The control system is designed to make the glider follow a continuously varying prescribed depth, or to maintain a constant depth.

The input to the system is a depth command voltage; this signal is compared to the depth signal which is provided by a pressure transducer in the glider. The difference signal, after some modification, generates the elevator deflection command. This excites the elevator control system, which also contains feedbacks, limiters and mechanical stop switches. A block diagram of the system is shown in Fig. 12.

The control system contains a number of buffer amplifiers, amplifiers working together to avoid a dead zone near zero input, summing amplifiers, power amplifiers and other components. In addition, since power and control signals are transmitted through a long cable, regulated power supplies and buffer amplifiers are needed in the glider as well as on deck.

Fig. 12 shows the depth command signal D_c being compared to the depth signal D_g originating from a pressure transducer in the glider. The difference is the depth error e. The depth control signal is related to the depth error by:

$$e_c(t) = K_c \left[K_e e(t) + K_1 \frac{de(t)}{dt}\right]$$

or, in terms of the Laplace transforms, c and e, they are related by the performance function:

$$e(s)/e_c(s) = \frac{1}{K_c(K_e + K_1 s)}$$

where s is the Laplace transform variable frequency.

Next the signal e_c, is limited, so as to generate an elevator deflection command $\tilde{e}_c$ within the usable range of elevator angle. The elevator command $\tilde{e}_c$ is compared to elevator angle e_Θ to generate the elevator error $e_{\Theta c}$. A power amplifier actuates the electric motor deflecting the elevator. A set of overtravel switches keeps the elevator from being jammed against its stops due to malfunctions elsewhere in the control system. The glider, responding to elevator deflections, will seek a

depth where the error signal e is zero. When the system operates within elevator command and elevator overtravel limits, the control system is linear. In order to close the loop, one needs to add the response of the depth D_g of the glider to elevator deflection Θ. This operator relating D_g and Θ is dependent upon depth, cable configuration and towing speed as well as other parameters. For small perturbations, the operator may be linear, but for example, at maximum depth, the relationship between D_g and Θ is definitely nonlinear.

Just imagine the extreme case when the towing cable is fully taut with the glider at its maximum depth. Then the glider will respond readily to a command to climb, but be unable to go deeper without pulling the stern of the towing vessel down. For small perturbations, about other states, the operator is linear. This approximate linear operator will contain the same terms for all parameter values and we have assumed that the coefficients in this linear approximation have the same sign for the whole range of parameter values.

This justifies the expectation that it is possible to use a linear constant coefficient control system. If the operator should change type when the parameters change, it would be necessary to use an adaptive servo. Such a servo would be much more complex than the present simple system.

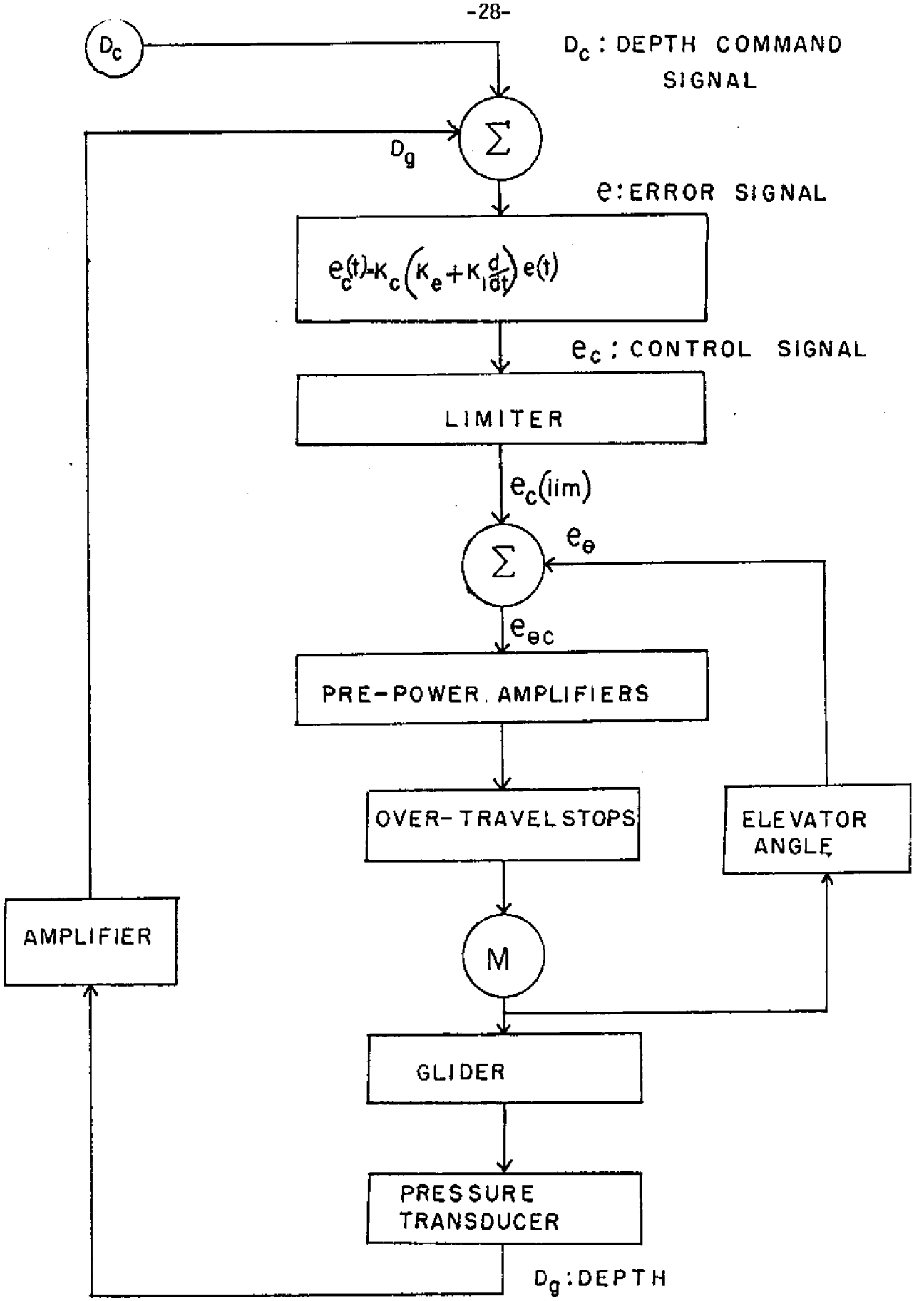

DEPTH CONTROL BLOCK DIAGRAM

FIG 12

9.0 Control system components

Each of the blocks described above will be described in detail below, starting with the depth command signal generator.

9.1 Depth reference signal circuit

The reference voltage D_c used as the input to the system is generated by the circuits shown in Fig. 13. When the glider is operated with the depth oscillating sinusoidally, a voltage D_{c1} from a low frequency oscillator is applied as input to amplifier A1b. The reference signal for keeping constant depth is generated by the potentiometers P1 (coarse control) D_{c2} and P2 (fine control) D_{c3}, buffered by the amplifiers A3a and A3b. The reference signals vary from -5v to +5v, corresponding to zero depth and 200 ft depth, respectively in the present design. The output from the pressure transducer in the glider is amplified to vary through the same voltage range as the reference signals and applied to buffer amplifier A1a. The output of A2a is the error signal e.

9.1.1 Input buffers

The input buffer amplifiers are dual integrated circuit amplifiers operated as voltage followers to provide isolation between signal sources. Fig. 13 gives the circuit diagram.

R_b provides a ground return for amplifiers A1a and A1b and prevents latch up if the input is either removed or interrupted.

9.1.2 Summing amplifiers

The outputs of the input buffers are the inputs to the second stage differential summing amplifier A2a. When all the summing and feedback resistors are closely matched in value and temperature coefficients, the output from A2a is proportional to the depth error D_g, and is applied as the input to the phase lead circuit that generates the elevator command signal.

9.2 Phase lead circuit

This circuit, shown in Fig. 13 generates the elevator command signal e_c by carrying out the operation:

$$e_c(t) = K_c\left[K_e + K_1 \frac{d}{dt} e(t)\right]$$

This is the input to the elevator angle control circuit.

9.3 Elevator angle control circuit

This circuit, located on circuit card #2 as shown in Fig. 14, provides feedback control and electronic limiting of elevator angle. The elevator command signal $e_{\theta c}$ is applied to the isolation resistor R11. The amplifiers A4a and A4b limit the signal to R9 at the summing ampli-

fier A3 to between $-E_{Ref}$ and $+E_{Ref}$. This prevents the circuit from attempting to deflect the elevator beyond preset limits, at the present time $\pm 22°$, corresponding to $E_{Ref} = 9$ v.

The elevator angular position feedback is provided by the potentiometer RT, which is geared to the elevator drive shaft. RT changes the feedback of the bridge amplifier A1. R1 serves to balance the bridge. R6 and R7 set the gain to provide an output voltage of ± 9 volts for $\pm 22°$ deflection.

The summing amplifier A3 will have a variable input, proportional to the elevator position error as long as neither of the amplifiers A4a and A4b clamps. If ec exceeds the limits, A4a or A4b will clamp and hold the input at R9 to ± 9 volts.

The output of A3 is applied to the servo preamplifier.

The voltage E_{Ref} shown is provided by a "Signetic dual polarity tracking regular".

9.4 Servo amplifier

Fig. 15 shows the servo amplifier and servo preamplifier; both are located on circuit card #3. The most important feature of the circuit is the compensation for the motor deadzone near zero input voltage. The preamplifier circuit "jumps the deadzone" by reacting to a change in input voltage polarity by generating an output voltage of changed polarity from A1b just sufficient to make the motor rotate.

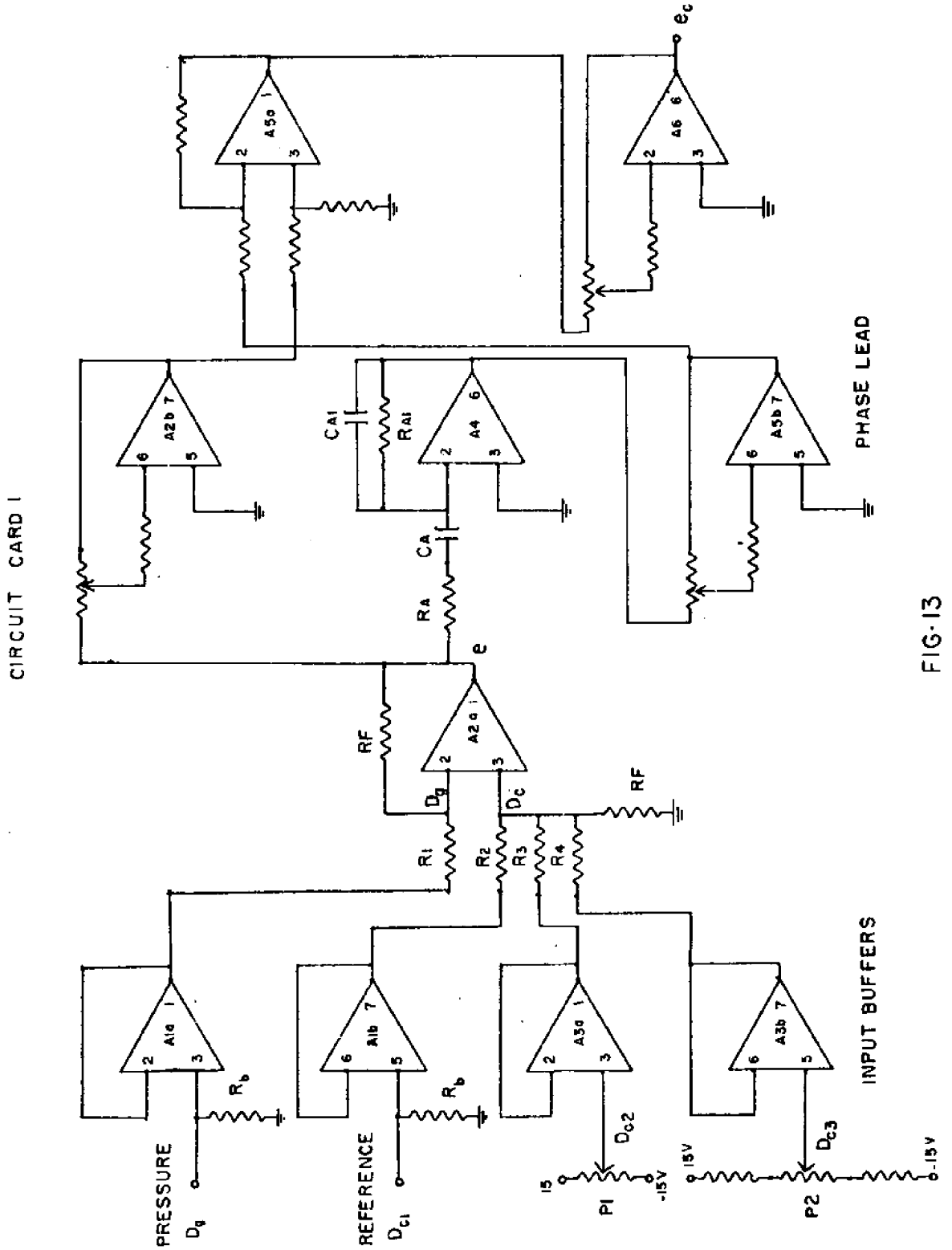
CIRCUIT CARD I
PHASE LEAD
INPUT BUFFERS
PRESSURE
REFERENCE
P1
P2
RF
RA
CA
CA1
RA1
R1
R2
R3
R4
Rb
15V
-15V

FIG-13

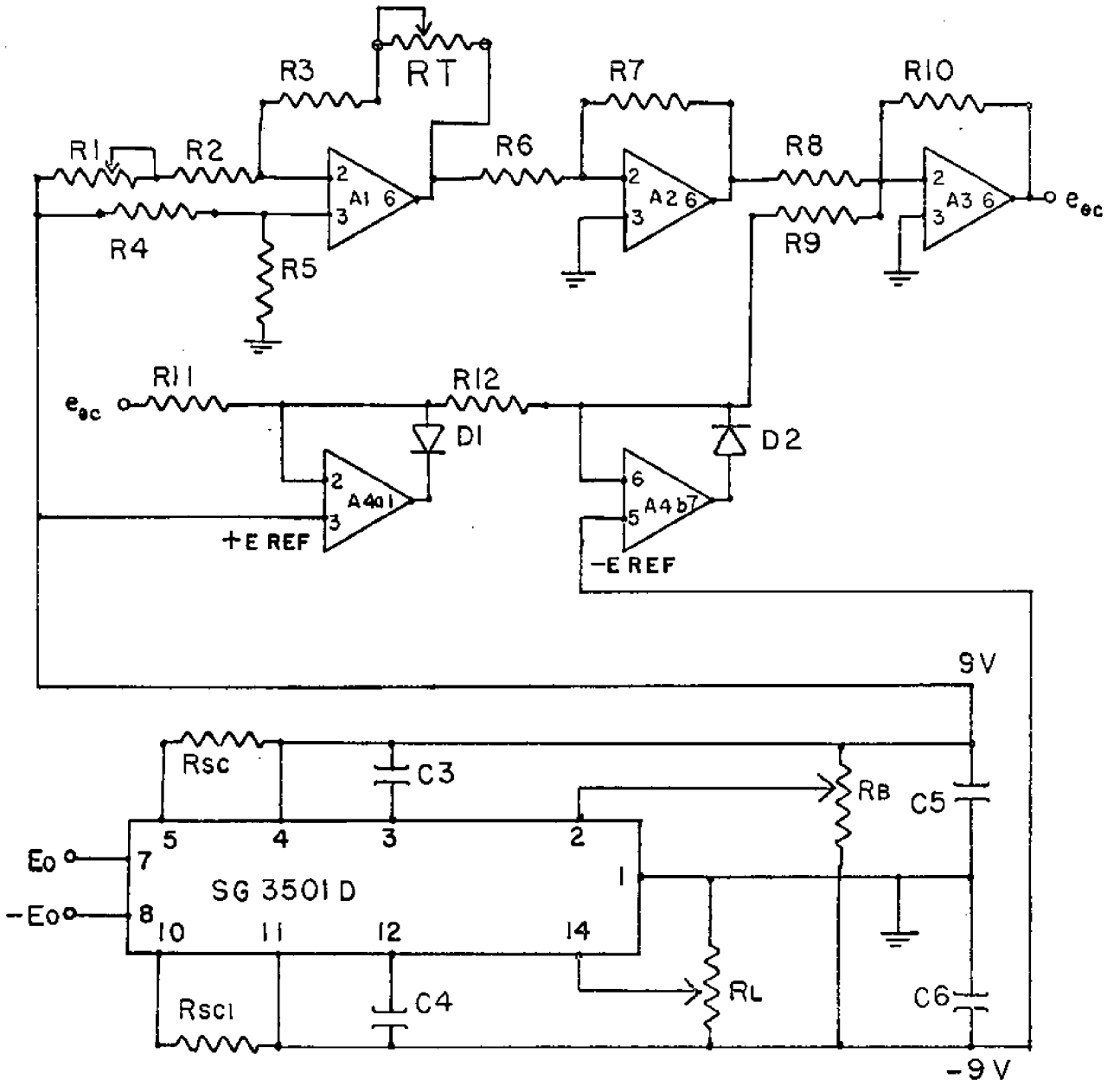

CIRCUIT CARD 2

ELEVATOR ANGLE CONTROL- LIMITER

FIG· 14

A1b also sums the normal error signal with the "jump voltage", providing proportional control with the dead zone eliminated.

Fig. 16a shows a schematic of the power amplifier stage. The circuit is designed to avoid any crossover dead zone when the input changes polarity. Class A-B biasing is used to eliminate the dead zone. The transistors Q1 and Q3 are connected in a basic complementary-symmetry output stage. The diodes D1 and D2 provide a forward bias to Q1 and Q3 even for zero input signal. Therefore, one transistor begins to conduct as the other approaches the turnoff point. The quiescent current is controlled by the current bias of the diodes D1 and D2, and by the relative voltage drops across the diodes, the base emitters junctions and across the resistors R_c and R_E.

The resistors R_{c1} and R_{c2} limit the power dissipation in the transistors. Diodes D5 and D6 contribute a more precise current limiting function. The circuit operates when the voltage $I_{01}R_{E1}$ becomes large enough to forward bias D5 into conduction. This shunts the current I_c to the level needed to keep diode D5 forward biased.

The schematic of the source of the constant current I_c (Fig. 16a) is shown in Fig. 16b. The actual circuit is shown in Fig. 15. The transistors Q1 and Q3 (Fig. 16a) have been replaced by conventional cc-cE transistor pairs Q2, Q3 and Q5, Q6 connected as emitter followers. This avoids having to use the original Q1 and Q2 as high gain CD transistor amplifiers.

CIRCUIT CARD 3

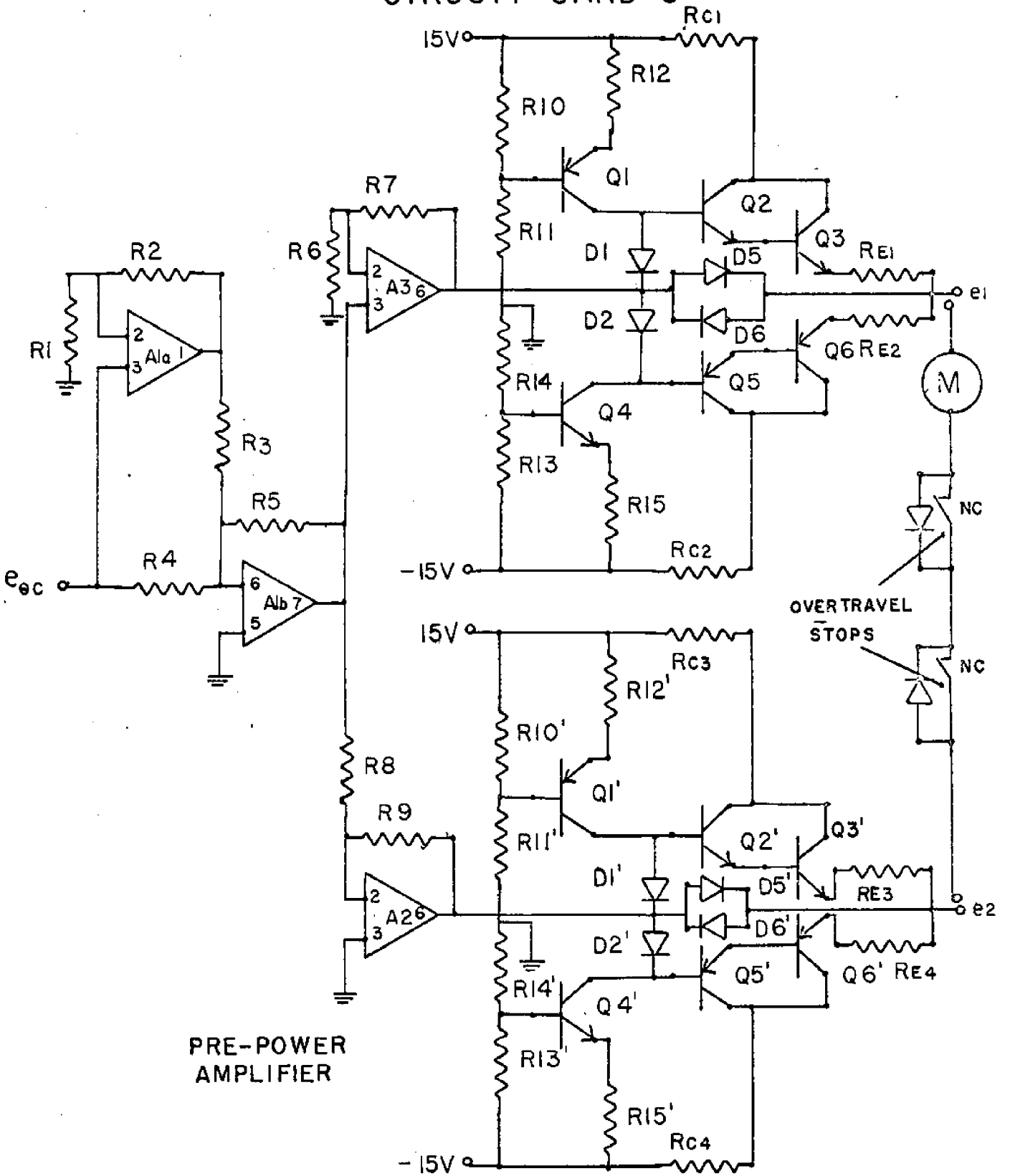

FIG·15

POWER AMPLIFIER

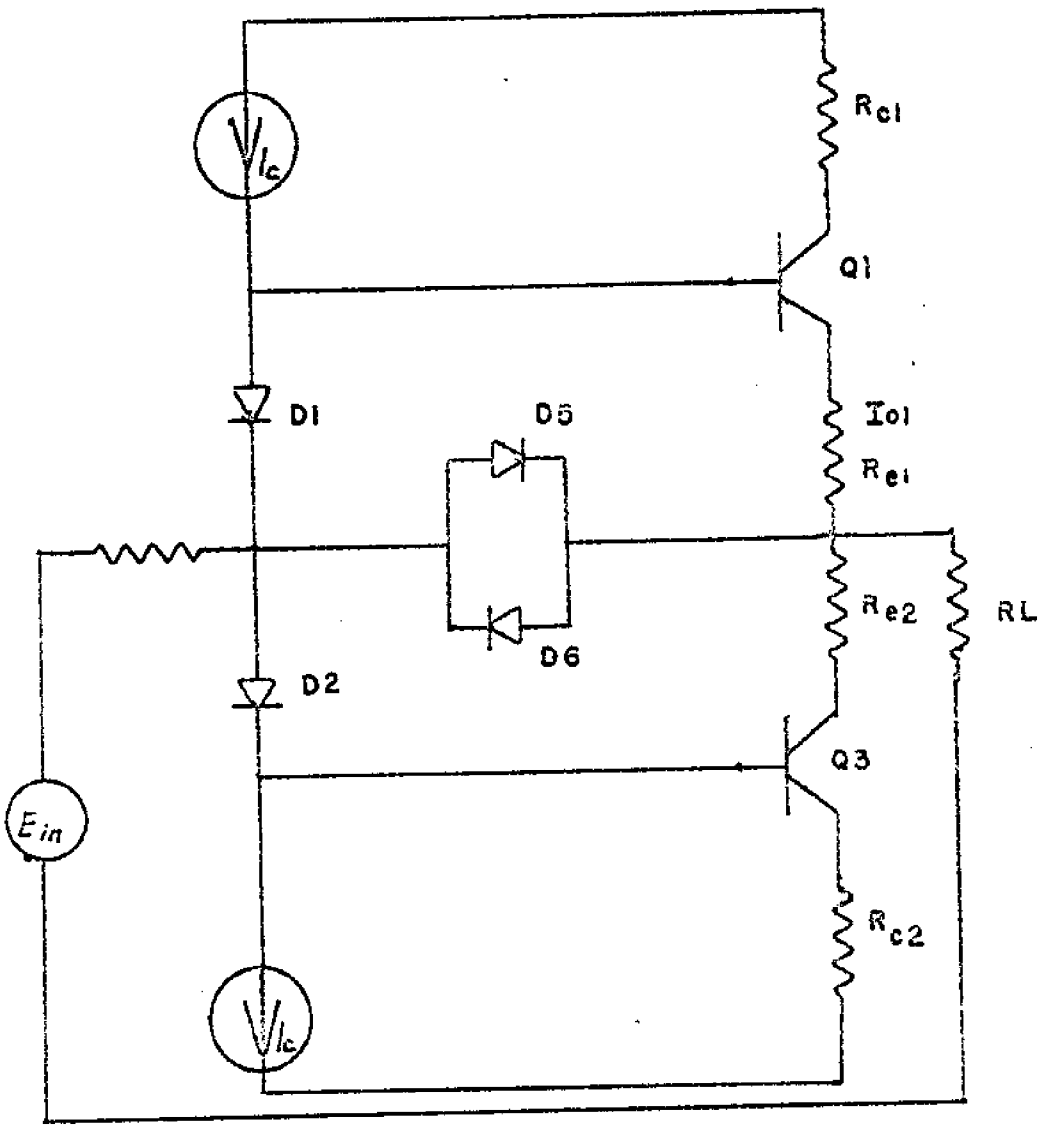

FIG. 16A

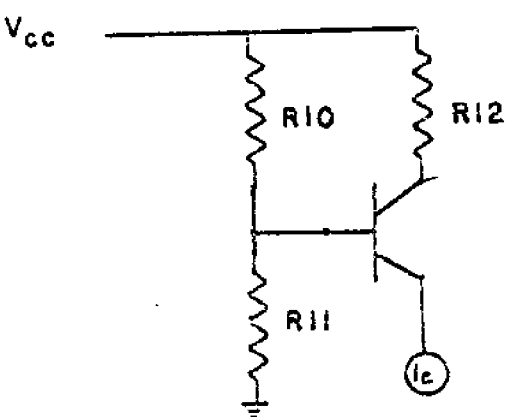

CONSTANT CURRENT SOURCE

FIG. 16B

The final circuit gives the high input impedance, low output impedance, high gain and wide frequency response needed in an amplifier to drive a servo motor. The use of a differential class A-B output stage doubles the output voltage swing and isolates the load from ground. Both are desirable features.

10.0 Power regulator card

The power to the transducer circuits in the glider are furnished by power regulators in the glider; these, in turn, are supplied with forty volts between the two leads in the towing cable that are available for this purpose. A "Lambda" power supply on deck feeds this pair of leads. The supply voltage requirements in the glider are:

±9 v for the Bathythermograph (BT)

±28 v for the voltage controlled oscillators in the BT, and for the Conductivity-Temperature-Depth (CTD) sensor package.

Fig. 17a shows the 27 volt (E_{02}) series regulator used to power a shunt regulator to provide both ±13 volts for the BT regulator and an artificial ground reference for the entire glider electronics system. The voltage E_{01}, when referenced to this artificial ground provides ±27 volts used for the VCO's and the CTD electronics. The Zener diode 21 is used as a shunt reference element to control the output Eo2 at 27 volts, which serves as the input to the shunt regulator. (Fig. 17b)

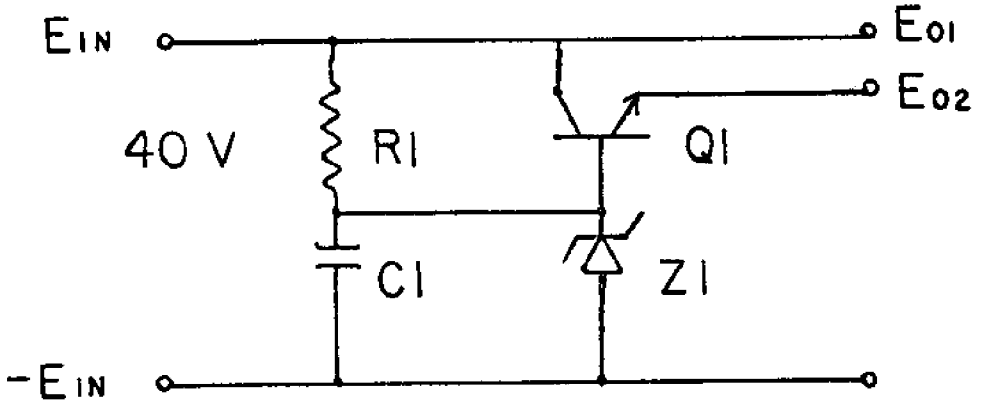

SERIES REGULATOR

FIG·17A

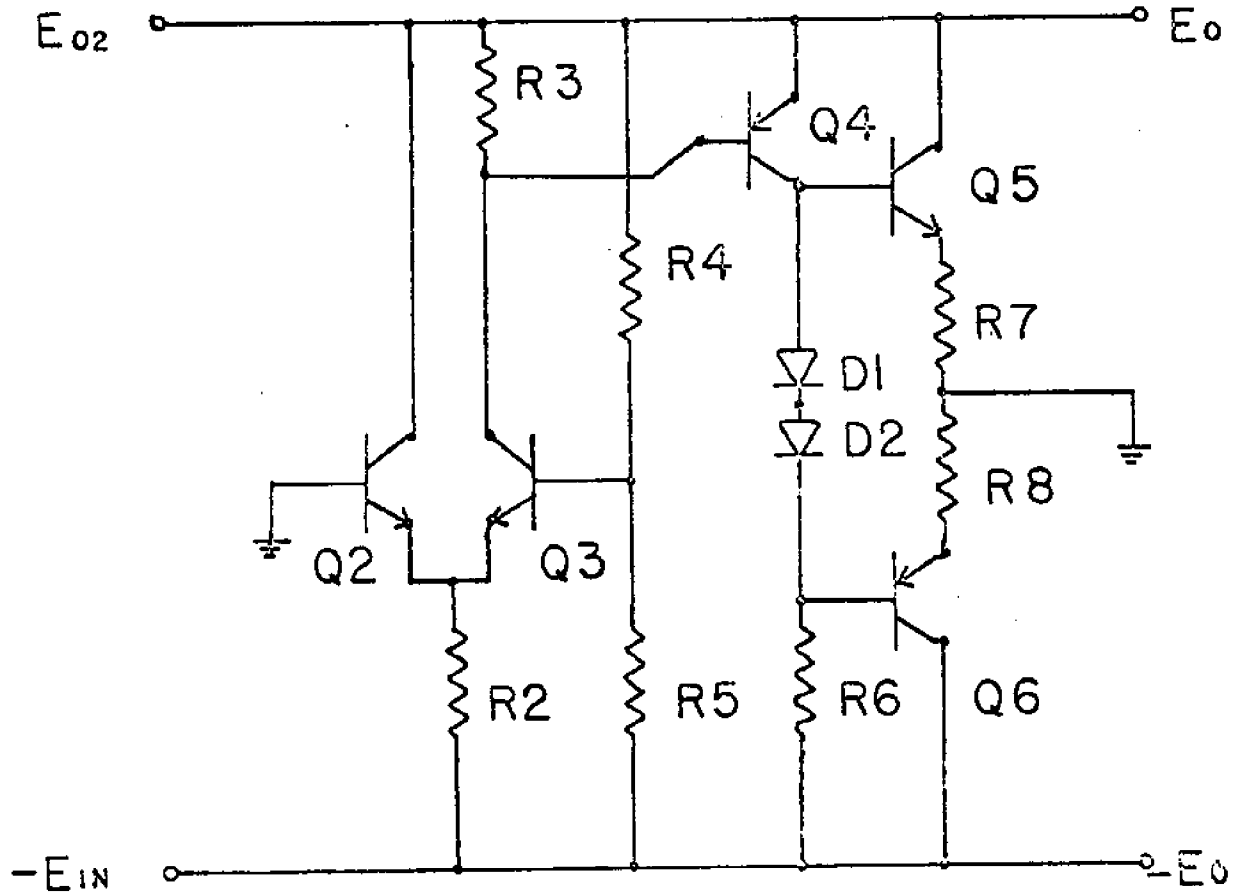

SHUNT REGULATOR

FIG·17B

The transistors Q1 and Q2 form a differential amplifier which compares the desired ground reference E_d to the artificial ground reference voltage E_a. The desired ground reference is chosen such that $+E_o$ and $-E_o$ will be equal and opposite. These are the inputs to the BT power supply.

10.1 Dual polarity tracking regulator

Fig. 18 shows the schematic of the Bathythermograph (BT) power supply, which consists of a dual polarity tracking regulator designed around a Silicon General SG 3501D integrated circuit. See Silicon General Applications Bulletin No. 1.

Additional current handling capability is provided through the use of external pass transistors Q1 and Q2. Resistors R_{sc} and R_{sci} are chosen on the basis of the relationship $R_{sc} = {}^{V_s}\frac{(tj\ max)}{I_{sc}}$ and provide output current limiting at 100 ma. Output voltage level adjustment is made possible by shunting the internal resistors, which set the negative output level by RL. A means of trimming output level differences is provided by R_B.

11.0 Field test results

The glider was first tested in Massachusetts Bay, and then used from R/V Columbus Iselin in the GATE III field study in late August and September, 1974. While a number of mechanical difficulties had to be over-

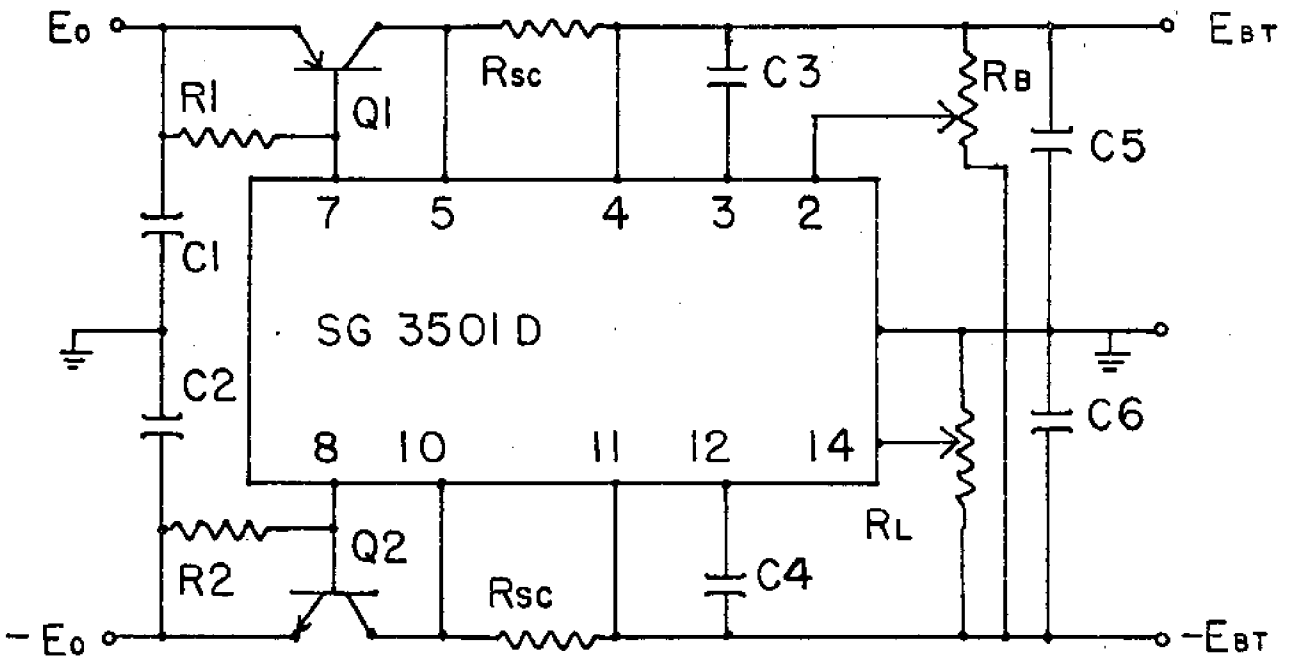

DUAL POLARITY TRACKING REGULATOR

FIG·18

come, at times by means of temporary fixes, the tests showed the glider to be capable of performing well, making useful observations.

Figures 19A through 21 show sample results from tests in Massachusetts Bay, carried out from the R/V R.R. Shrock, a fifty foot vessel. Fig. 19 shows depth versus time for several settings of feedback gains. Tests were carried out in five foot waves and the results are shown in Fig. 20. Note that the glider depth variation in Fig. 21 is less than one foot.

Fig. 22 shows a segment from the GATE III data of depth and temperature outputs from the CTD and the BT while towing at a depth of 95 feet in the level operating mode. Note how the temperature outputs agree. The event appears to be a combination of internal waves of three distinct wavelengths, the smaller ones riding on the larger ones. Fig. 23 shows conductivity, temperature and depth traces while operating in an oscillatory mode with "bang-bang" control (full up elevator, then full down elevator). This run, from early morning, apparently shows the inversion in conductivity resulting from night-time convection induced by radiative sea surface cooling. These analog sample outputs are mainly for monitoring and preliminary data assessment. The working data are being processed digitally.

12.0 Suggested modifications

The principal need for modification is in simplifying and ruggedizing the horizontal tail assembly. The actuator motor has plenty of power, and

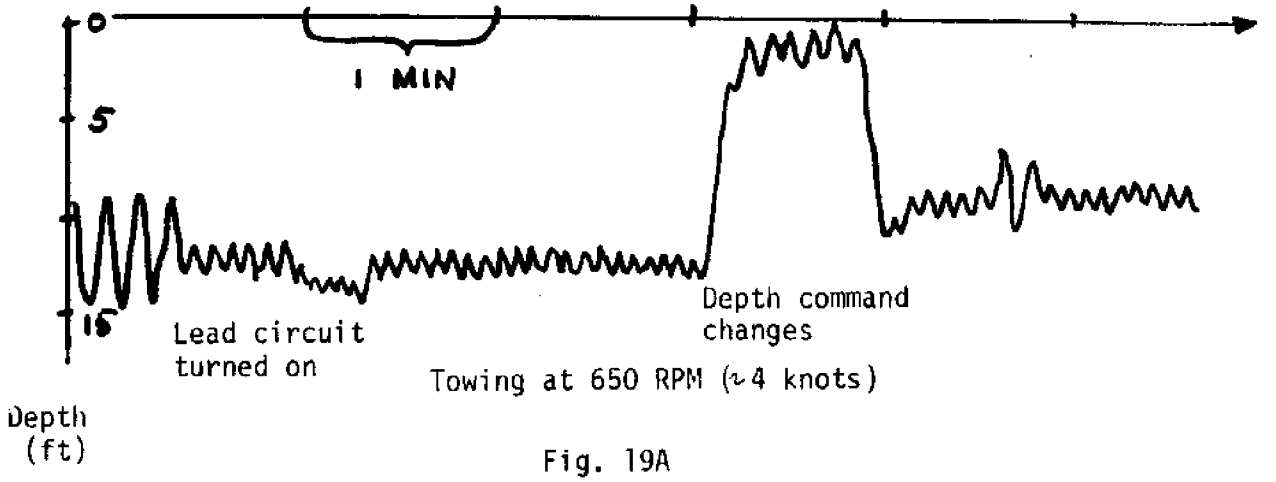

Fig. 19A

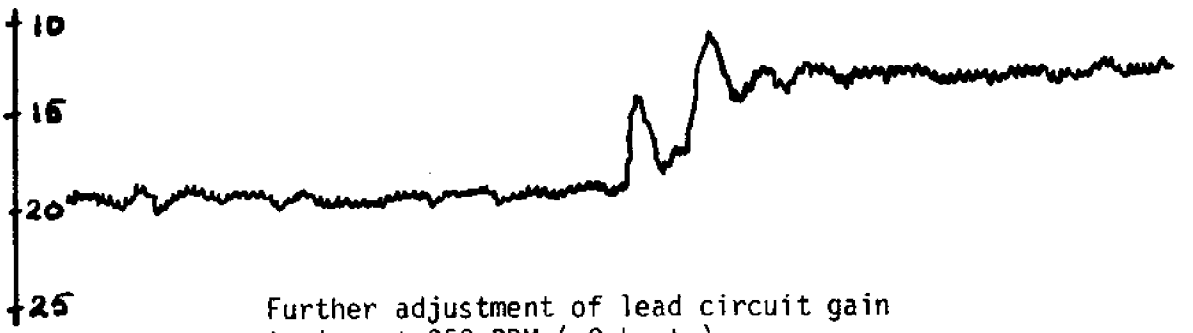

Fig. 19B

Fig. 19 Depth of glider versus time, showing effect of lead circuit gain.

Tow cable length 46 feet.
Depth range 0-28 feet.
Elevator stops at ±30°.

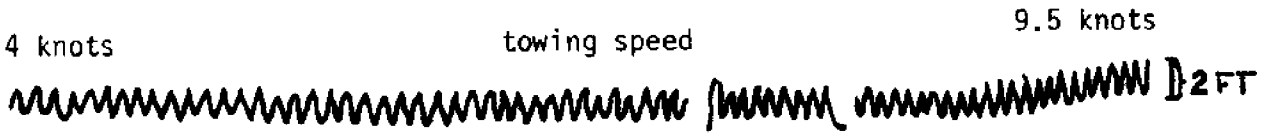

Fig. 19C

Change in glider oscillation frequency with gradual change in towing speed.

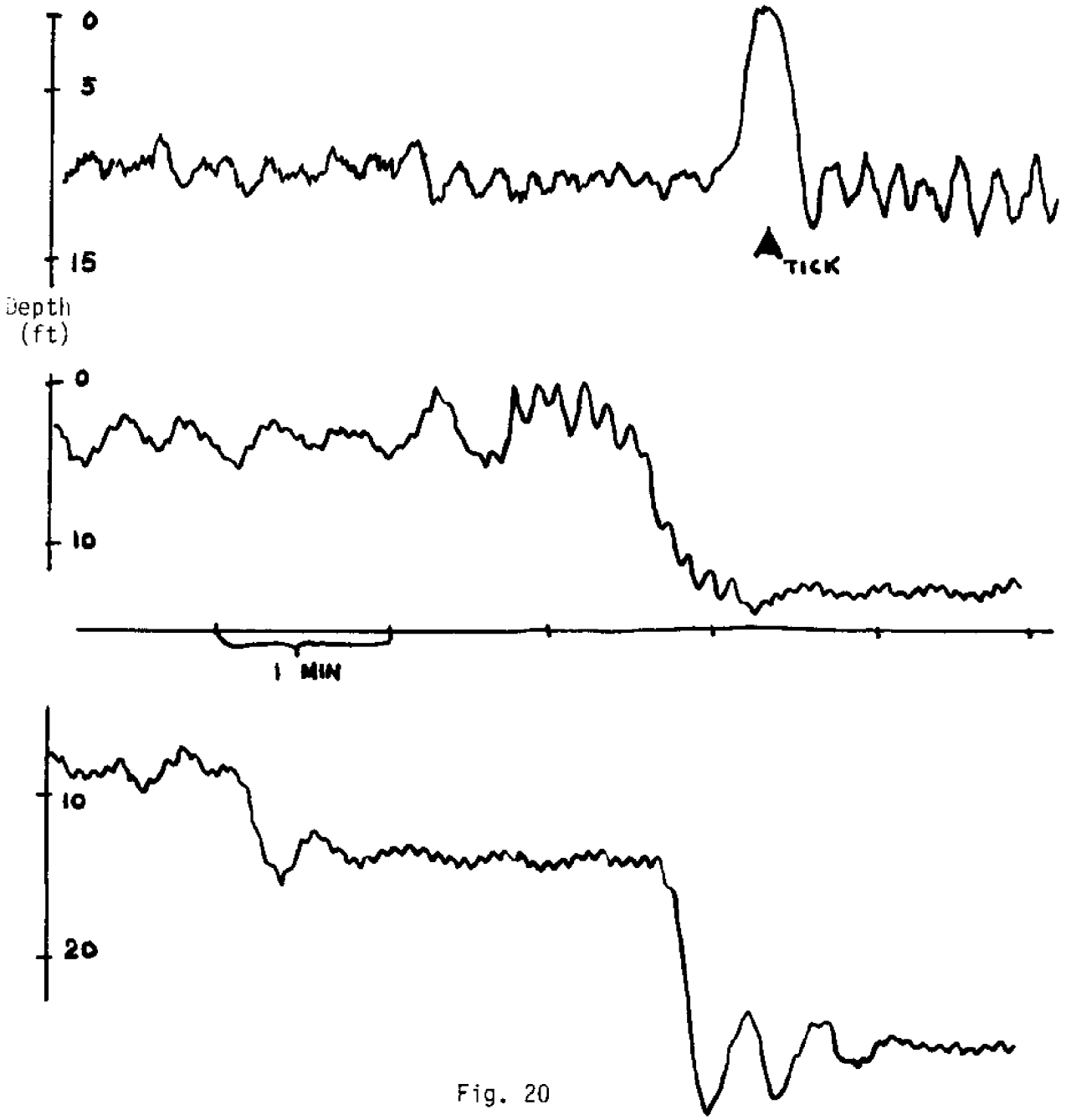

Fig. 20

Glider depth (in feet) versus time towing in five foot seas using 50 foot towing vessel. Upper trace tick marks where towing cable length was increased from 46 feet to 86 feet. Middle and lower traces show that increasing depth decreases response to waves.

Fig. 21

Depth control system performance after final circuit cleanup. Cable length 46 feet, towing at ~4 knots, average depth 18 feet.

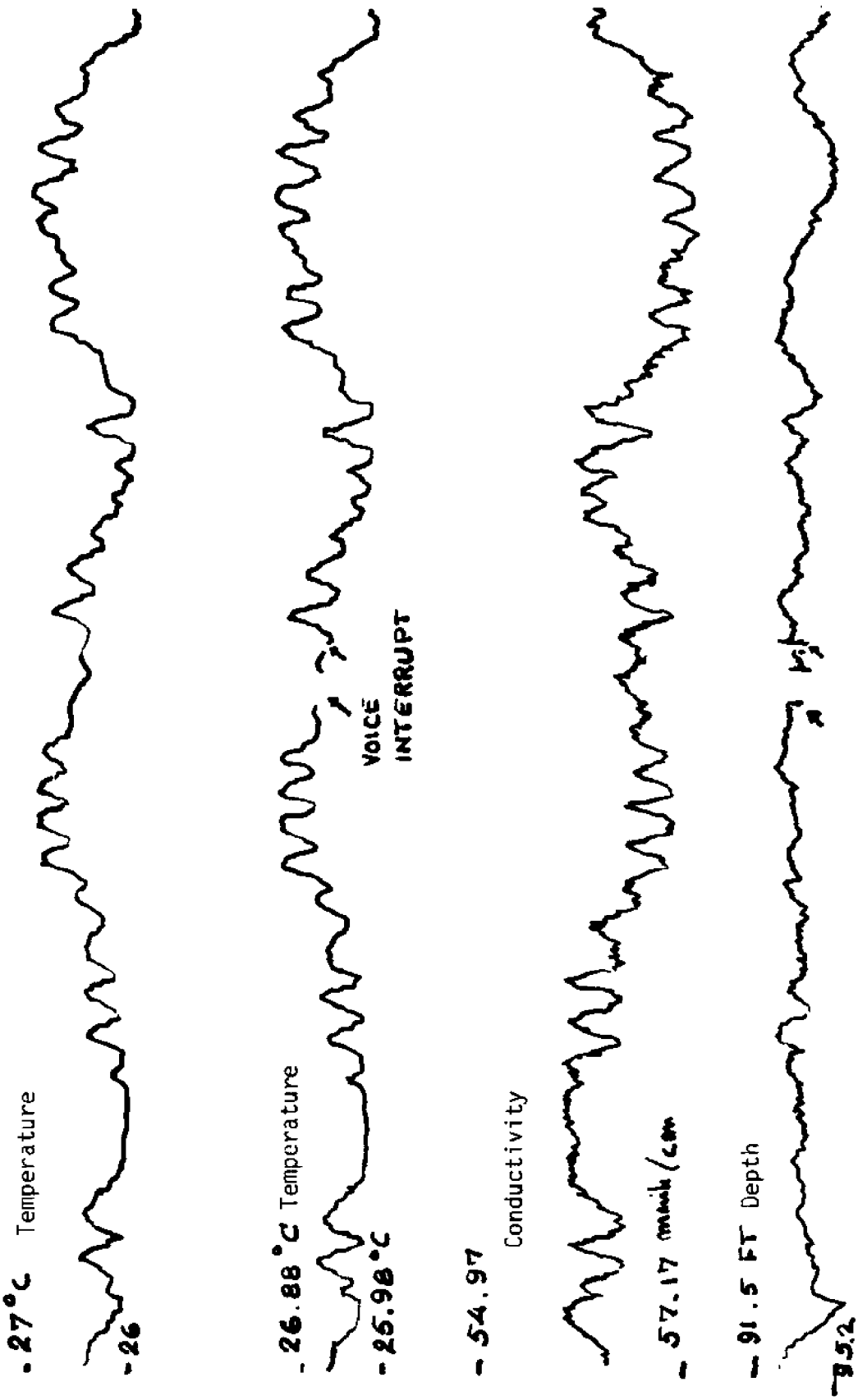

Fig. 23 Temperature from CTD (upper trace) from BT (second trace) and conductivity (third trace) and depth versus time during a "constant depth" tow in GATE III.

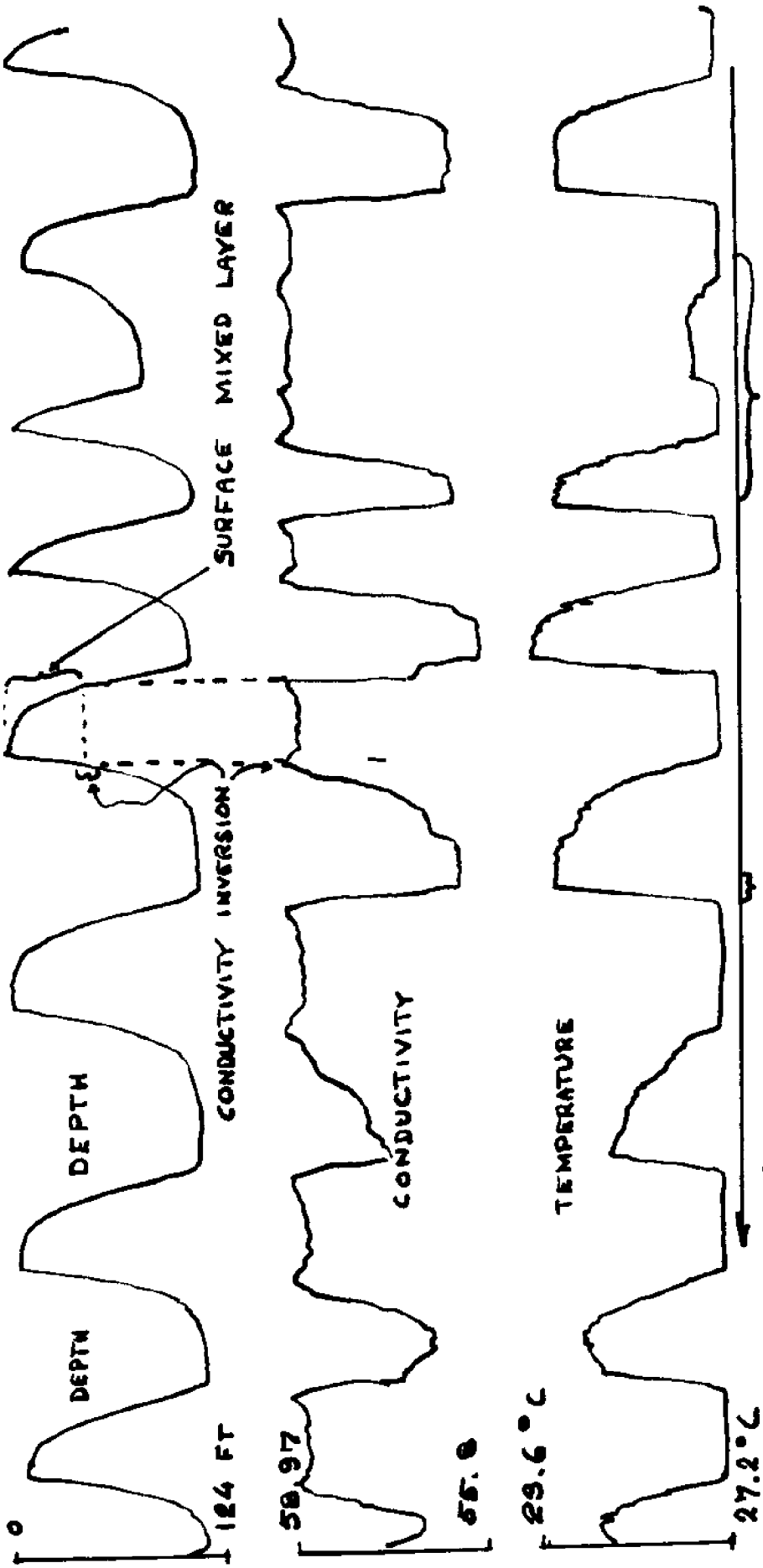

Fig. 23 Analog traces of depth (upper trace), conductivity (middle trace) and temperature (lower trace) obtained during GATE III. Data from night-time tow, showing conductivity inversion layer probably caused by night-time convective overturning.

we suggest that a fixed horizontal tail with a conventional elevator be used. Then more rugged dimensions can be used for the elevator shaft and actuator gears. At the same time, hand-holds can be arranged directly on the horizontal stabilizer.

The other troublesome element was that the electrical connector between the glider and the towing cable was exposed to the flow. The resulting vibration damaged the leads at the crimped connections. An improved cable electrical lead-in is clearly necessary.

Otherwise, the glider design is ready to be cleaned up with some additional streamlining of the tubular bumpers, replacement of nuts and bolts with stainless where stainless parts were not available at the last moment before the glider was due to be shipped to Dakar to be put on board the ship.

With these modifications, the present glider appears to be a useful observational tool in oceanography. In addition the present glider will prove useful in the development of improved prototype designs, serving as a test platform and as a test vehicle for design concepts and features. We do not recommend that the present glider serve as a prototype for procurement of many gliders.

If anybody should want to copy the present design, they are of course free to do so. We suggest that it may be both cheaper and more effective for prototype development to be carried out by an outfit with both

engineering capability and production experience. The next step, in our opinion, would be for an agency of the Government to invite bids for a prototype design and delivery and demonstration of an instrumented prototype.

13.0 Conclusion

A towed glider with automatic depth control is a feasible and useful tool in surface layer oceanography, according to performance tests and field tests of the "Hydroglider". With some modification, it will be suitable for routine use. Replication for wider use and series production may have to await final engineering of a prototype.

Appendix I

"Using a Dual Polarity, Tracking Voltage Regulator"

(Silicon General Applications Bulletin No. 1)

Silicon General
LINEAR INTEGRATED CIRCUITS

APPLICATIONS BULLETIN NO. 1

USING A DUAL-POLARITY, TRACKING VOLTAGE REGULATOR

Robert A. Mammano
Silicon General, Inc.

INTRODUCTION

Voltage regulator applications have long represented a challenge to the monolithic integrated circuit designer as the development of practical devices has necessitated solutions to several very difficult problems. Among these are obtaining high current capability in monolithic transistors, developing temperature compensated reference elements and accurate current sources, and combining critical error sensing circuitry on the same chip with high power components. The versatile positive and negative regulators which are available today are a credit to their designer's skills in solving these knotty problems.

A single dual-voltage regulator, however, while long recognized as a needed component for most analog systems, has presented even greater difficulties. Not only must one build two complete regulators as one device — the design must be compatible with the power dissipation and pin limitations of available low-cost IC packages. In addition, positive and negative circuitry requires complementary devices which, until recently, were unavailable in monolithic form.

In the development of the SG1501, solutions have been found to these problems and the result is the industry's first fully monolithic dual-polarity voltage regulator.

CIRCUIT OPERATION

The basic operation of the SG1501 is best visualized through the block diagram shown in Figure 1. The circuit is fundamentally a tracking regulator. That is, the negative voltage is regulated and the positive output tracks the negative. Negative regulation is accomplished by providing a constant-voltage reference for the negative error amplifier, but the reference input to the positive error amplifier is grounded. This amplifier forces its other input, which is the center-tap between equal resistors, to also be at zero volts, thus requiring the positive output to be equal in magnitude but opposite in polarity to the negative output.

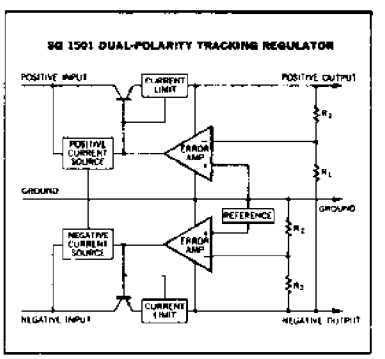

Figure 1. Block Diagram

With this technique, a single adjustment of the negative voltage divider, which changes the negative output level, will also provide exactly the same change to the positive output voltage. This tracking will hold all the way from approximately one volt above the reference voltage, to a maximum value of about one volt less than the input supply voltage.

The SG1501 differs from the other IC voltage regulators in that the error amplifiers are driven from the regulated output voltage rather than from the input. While this does limit the minimum output voltage, it also provides extreme stability for error sensing. The result is a voltage regulation 10 to 100 times better than previously available.

From the schematic of Figure 2, it can be seen that there are several other differences in circuit techniques over past IC designs. The most obvious is the use of complementary PNP transistors. These are lateral types and while they still have some current and frequency limitations, processing advances have increased their current gain from the usual 2 to 4 range up to between 50 and 100, greatly simplifying circuit design. Another process development, the compatible FET, shown as Q2, provides a current source almost completely unaffected by input voltage variations which further adds to the output voltage stability.

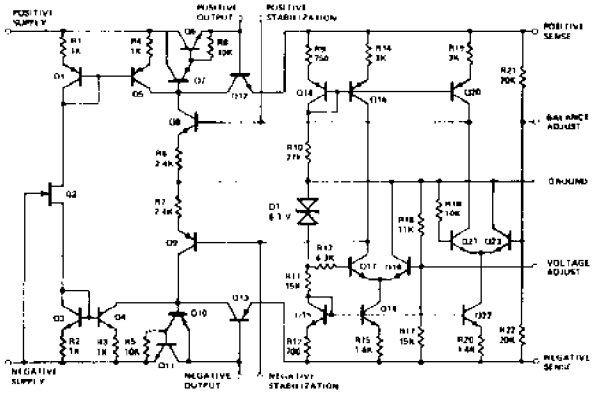

Figure 2. Schematic Diagram

The excellent temperature performance of the SG1501 results largely from the development of a zero TC reference element. While older designs were able to get low temperature coefficient reference voltages, it was accomplished by combining several temperature sensitive elements in a self-compensating arrangement. While this approach could accommodate external ambient temperature variations, thermal gradients caused by internal device heating would upset the compensation and cause relatively large output shifts. Since the reference in the SG1501 is a single component, no compensation is required and a stable output is maintained regardless of either absolute temperature or thermal gradients.

As the SG1501 was designed specifically for ±15 volt outputs, it was decided to include the voltage sensing resistors in the monolithic chip – another departure from conventional IC regulator design. If not carefully done, this could cause problems due to the temperature coefficient of diffused resistors; however, the geometric design of these components was defined in such a way as to optimize their tracking regardless of thermal gradients within the chip.

Since modern processing technology has significantly enhanced the components available to the IC designer, it was possible to use a very straight-forward over-all circuit design for the SG1501. An examination of the schematic of Figure 2 will show a general approach well proven in past discrete component designs. The error sensing amplifiers are matched differential amplifiers with current-source collector loads for maximum gain. Transistors Q8 and Q9 are included primarily as level shifters to isolate the output voltage from the collectors of the diff amps, but they also provide additional gain and thus contribute to the superior regulation characteristics of the SG1501.

While the positive pass transistor is a conventional Darlington NPN pair, high current PNP transistors still elude the monolithic designer. Thus the negative power device is a compound pair with an NPN unit serving as the primary current amplifier. The result is a simulated power PNP transistor which, while not able to pass the same maximum current as the all – NPN device, has superior saturation characteristics at lower currents. The best comparison of the two series pass elements of the SG1501 is shown in the minimum input-output voltage differential curves of Figure 3.

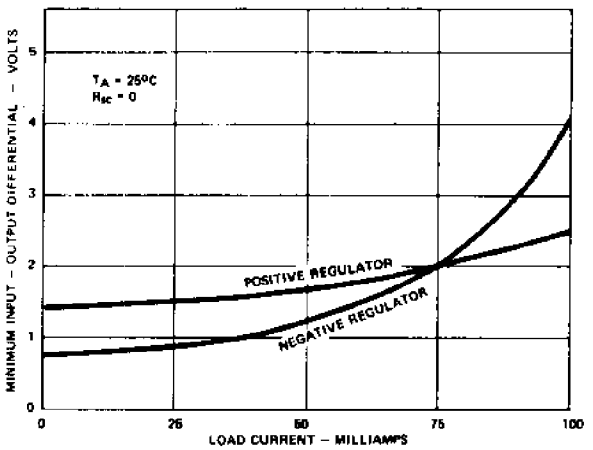

Figure 3. Regulator Dropout Voltage

As a final note on the design of the SG1501, mention should be made of the circuit layout shown in the photo micrograph of Figure 4. This chip, with a size of 71 x 50 mils, was organized specifically for maximum thermal performance. The power devices were separated from the critical error sensing circuitry and both the differential amplifier and sensing resistors were laid out according to the temperature isotherms. Thus the output voltage is almost totally insensitive to internal power dissipation.

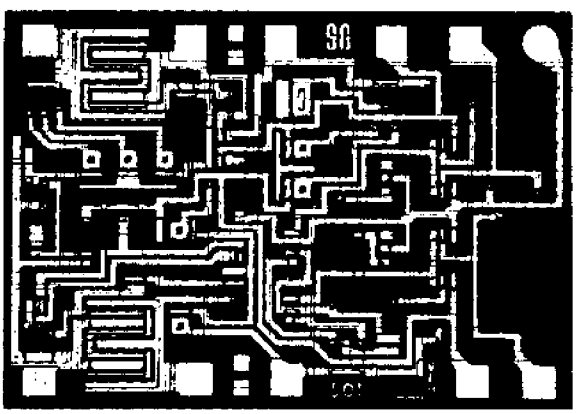

Figure 4. SG1501 Photo Micrograph

Appendix II

Additional illustrations

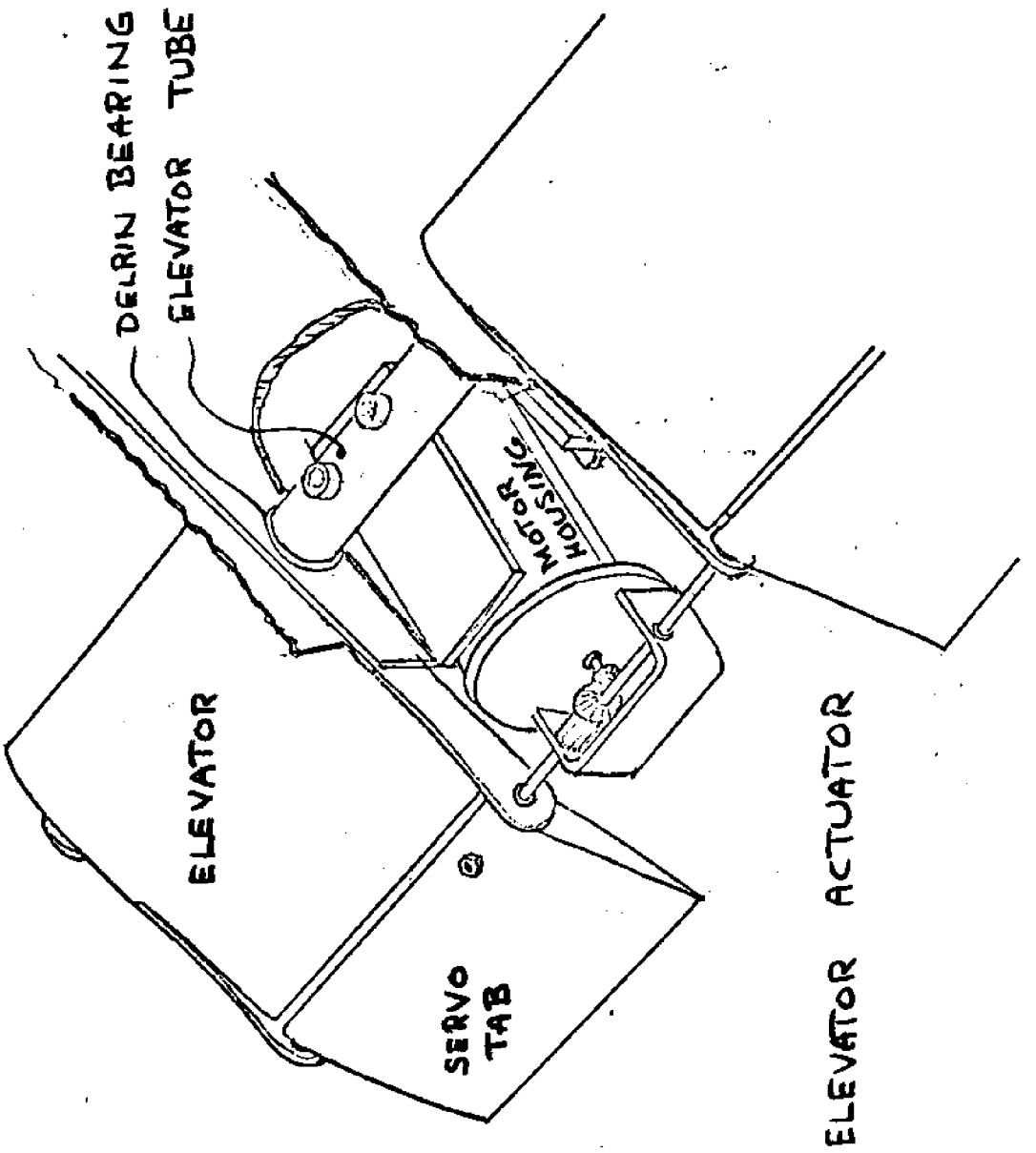
DELRIN BEARING
ELEVATOR TUBE
MOTOR HOUSING
ELEVATOR
SERVO TAB
ELEVATOR ACTUATOR

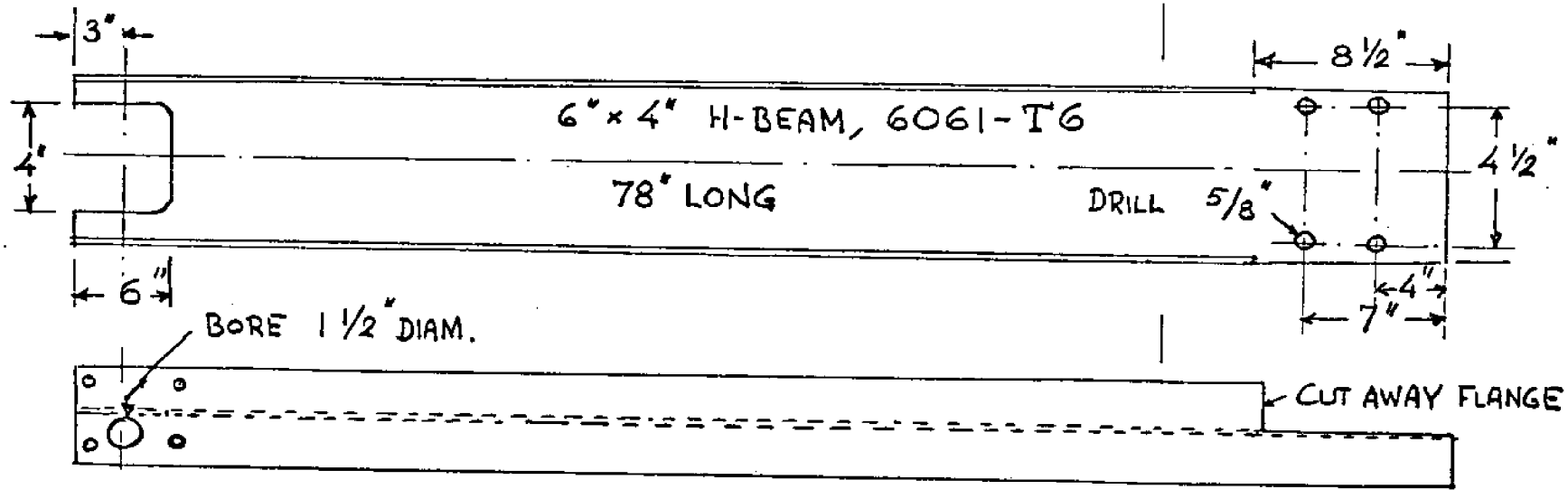

FUSELAGE BEAM

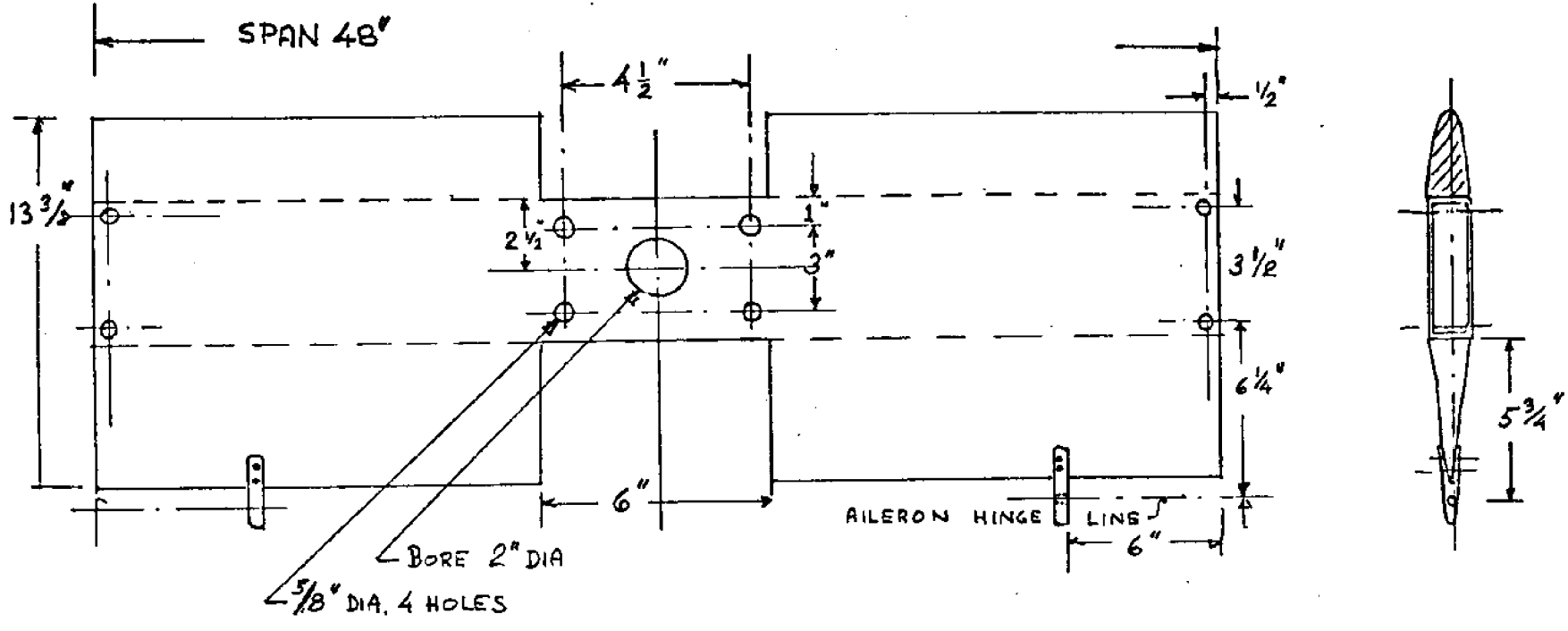

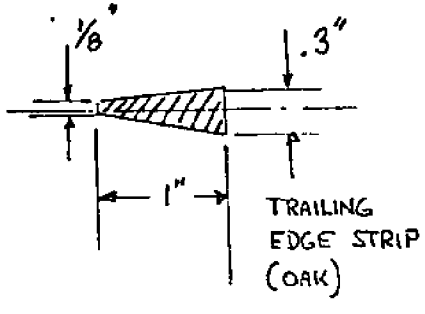

WING PLANFORM & CONSTRUCTION

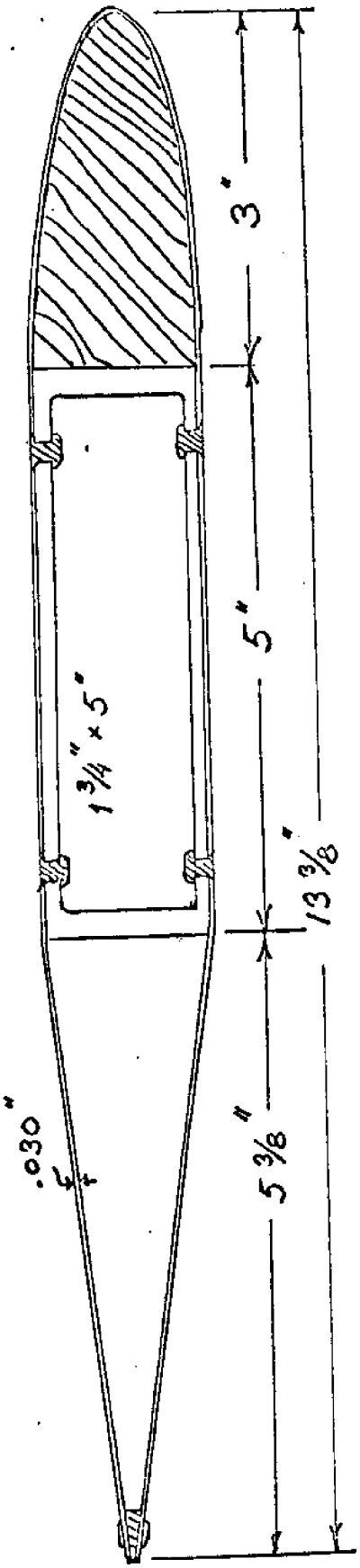

WING SECTION

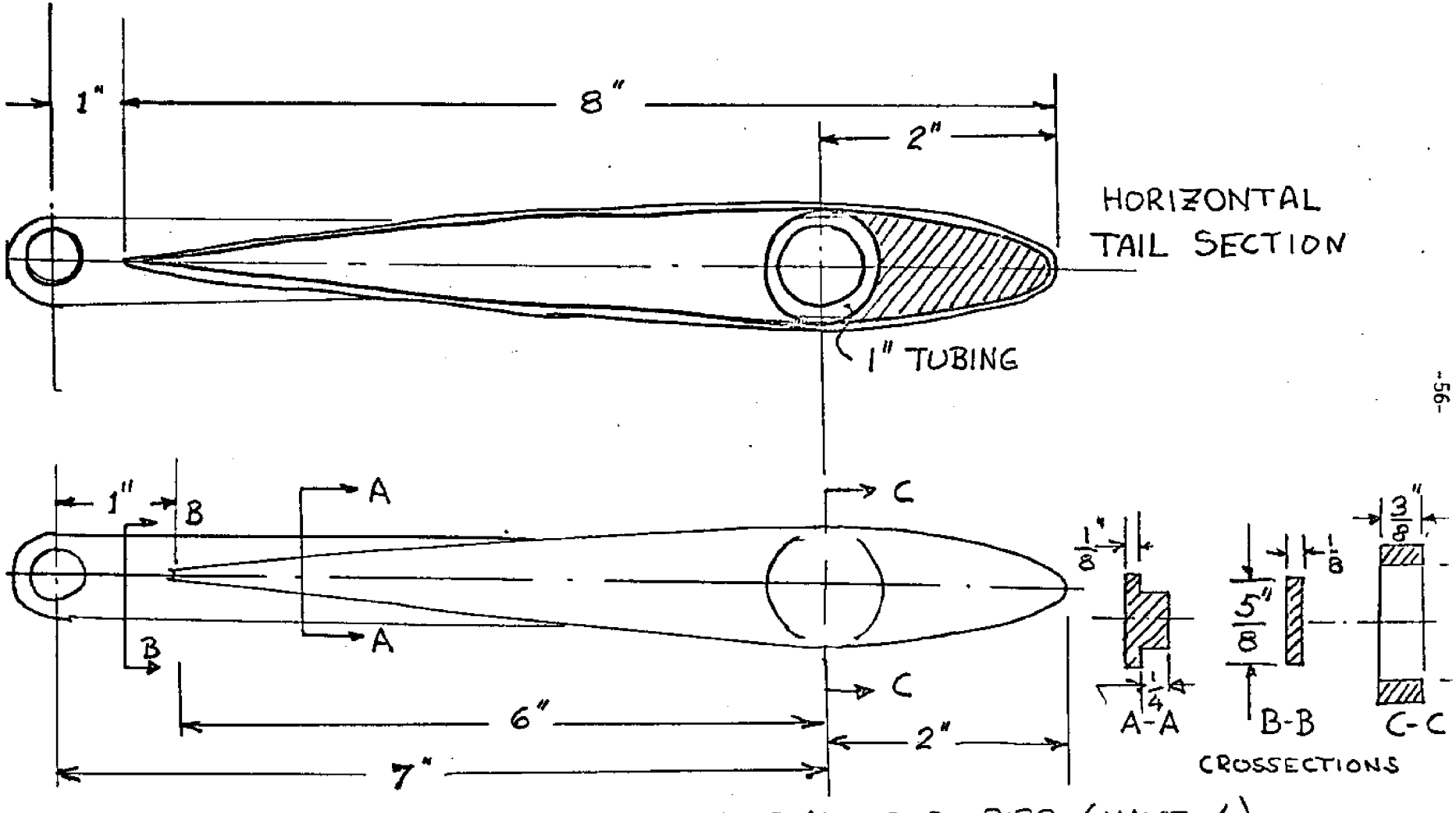

HORIZONTAL TAIL END RIBS (MAKE 4)

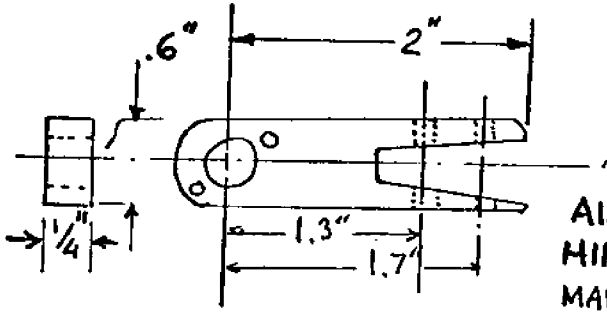

AILERON
HINGE BRACKET
MAKE 2.

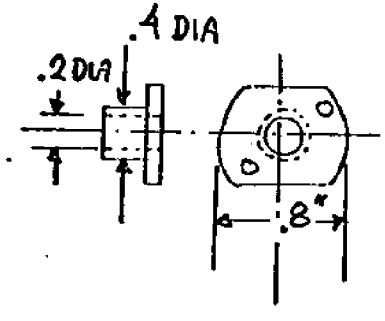

BEARING INSERT IN TIPTANK
MAKE 4. DELRIN

AILERON BEARINGS

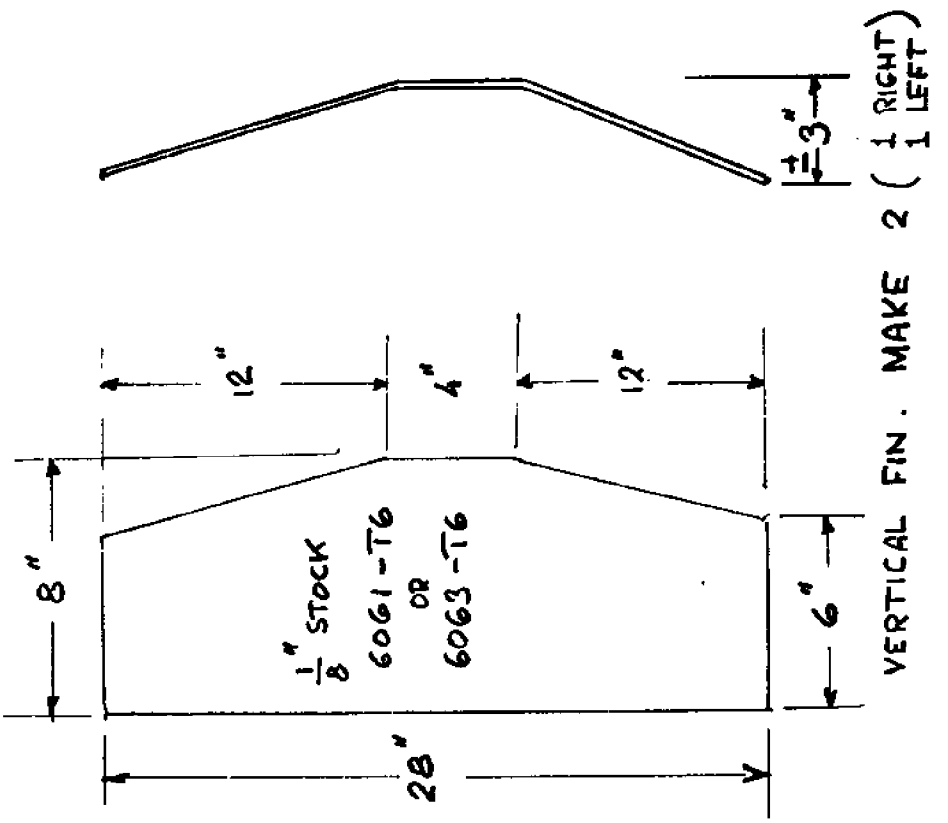

VERTICAL STABILIZER

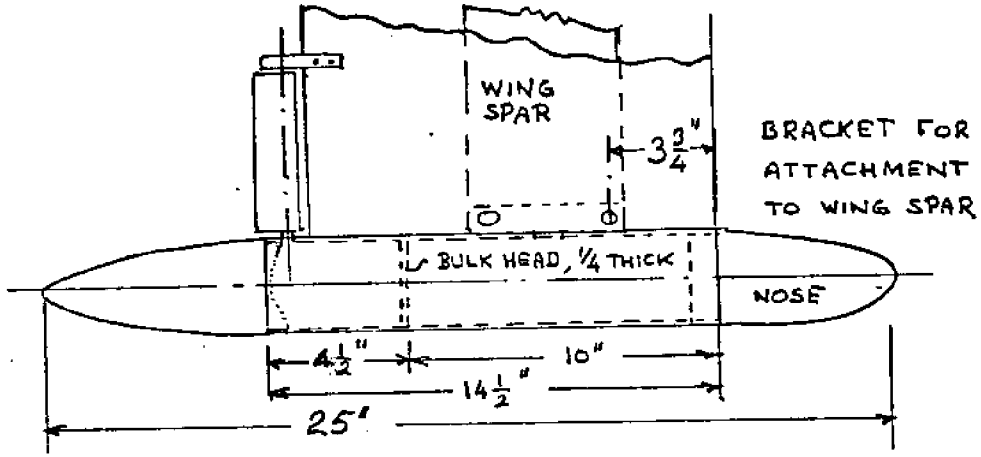

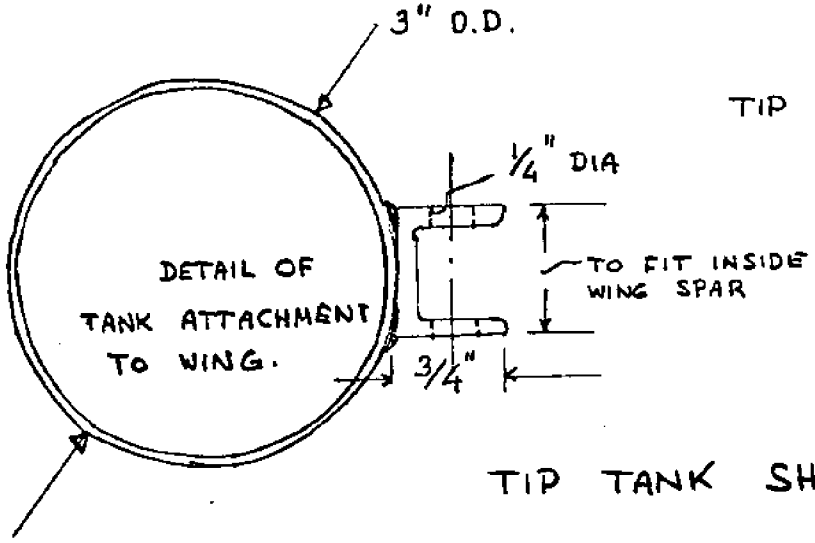

TIP TANKS.

TIP TANK SHELL DESIGN

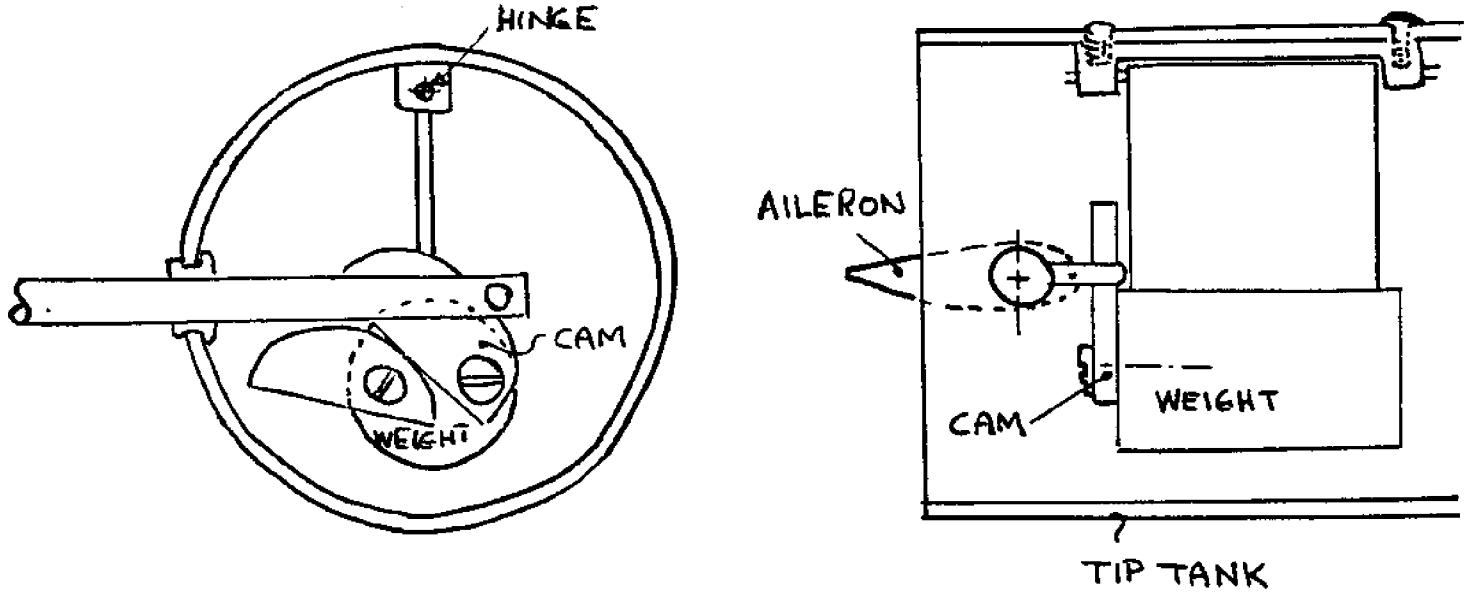

AILERON CONTROL PENDULUM

APPENDIX III

On-deck Recording System

The depth temperature and conductivity signals from the CTD and the BT packages in the glider are all in FM format. On the deck of the towing vessel the terminal equipment is housed in two metal cabinets. (Fig. 1)

The FM signals are recorded as received from the glider on a Hewlett Packard (HP) 3960 series tape recorder for digital processing upon return to M.I.T. The signals are also discriminated (FM to analog conversion) amplified and plotted on an HP xy_1y_2 recorder for "quick" look to ensure that reliable data are being recorded. An HP strip chart recorder is used to monitor the depth signal. Fig. 2 shows a block diagram of the on board recording equipment.

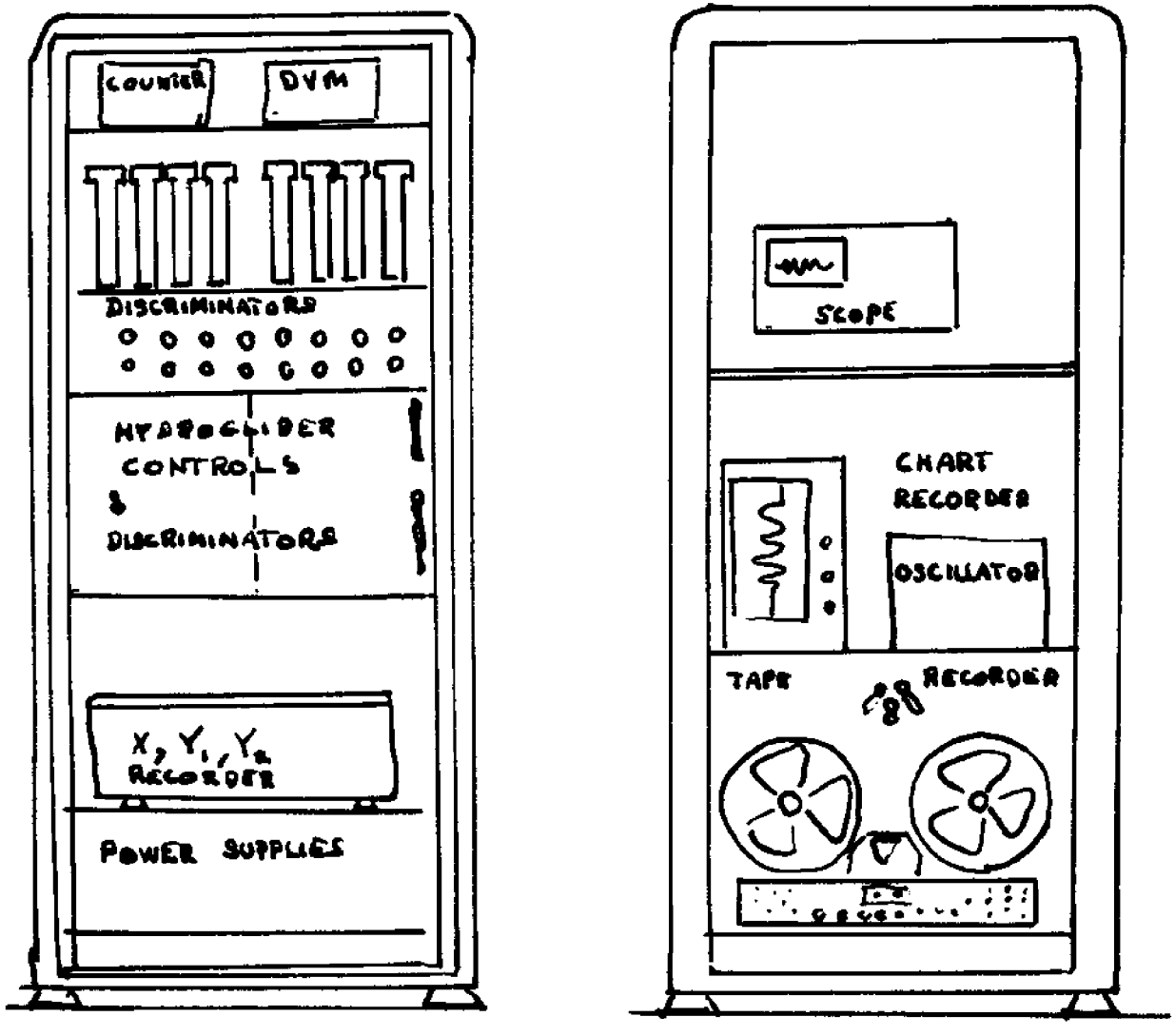

On Board Equipment Arrangement

Rack Mounted

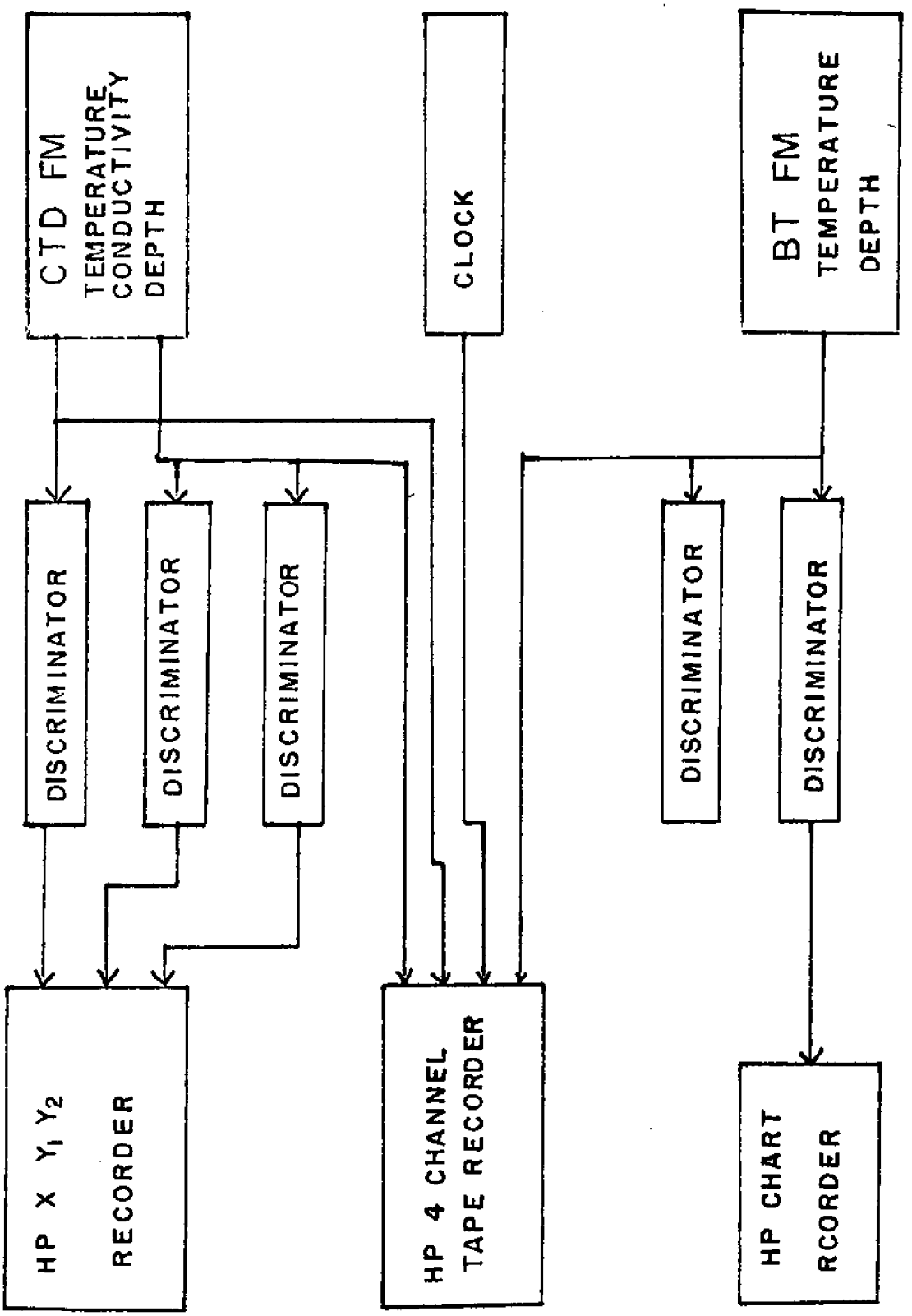
CTD FM
TEMPERATURE
CONDUCTIVITY
DEPTH
CLOCK
BT FM
TEMPERATURE
DEPTH
DISCRIMINATOR
DISCRIMINATOR
DISCRIMINATOR
DISCRIMINATOR
DISCRIMINATOR
HP X Y1 Y2
RECORDER
HP 4 CHANNEL
TAPE RECORDER
HP CHART
RCORDER
ON BOARD RECORDING

FIG·2